

Force-Induced Calcium Concentration Change and Focal Adhesion Translocation:
Effects of Force Amplitude and Frequency

by

Peter J. Mack

B.S., Mechanical Engineering (2002)

University of Notre Dame

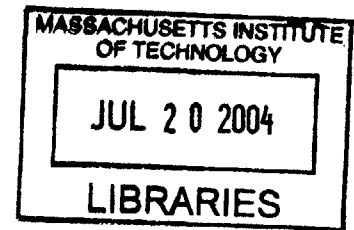
Submitted to the Department of Mechanical Engineering
in Partial Fulfillment of the Requirements for the Degree of
Master of Science in Mechanical Engineering

at the

Massachusetts Institute of Technology

June 2004

© 2004 Massachusetts Institute of Technology
All rights reserved



Signature of Author.....

.....
Department of Mechanical Engineering
May 7, 2004

Certified by.....

.....
Roger D. Kamm
Professor of Mechanical Engineering
Thesis Supervisor

Certified by.....

.....
Dr. Richard T. Lee
Department of Medicine, Brigham and Women's Hospital
Thesis Supervisor

Certified by.....

.....
Mohammad Kaazempur-Mofrad
Research Scientist in Mechanical Engineering
Thesis Supervisor

Accepted by.....

.....
Ain A. Sonin
Chairman, Department Committee on Graduate Students

BARKER

FORCE-INDUCED CALCIUM CONCENTRATION CHANGE AND FOCAL ADHESION TRANSLOCATION: EFFECTS OF FORCE AMPLITUDE AND FREQUENCY

by

PETER J. MACK

Submitted to the Department of Mechanical Engineering
on May 7, 2004 in partial fulfillment of the
requirements for the Degree of Master of Science in
Mechanical Engineering

ABSTRACT

Vascular endothelial cells rapidly sense and transduce external forces into biological signals through a process known as mechanotransduction. Numerous biological processes are involved in mechanotransduction, including calcium signaling and activation of focal adhesion sites, but little is known about how cells initially sense changes in the external mechanical environment.

In order to examine the rapid mechanosensing thresholds involved with mechanotransduction, calcium concentration changes and focal adhesion site translocations were observed while applying nN-level magnetic trap shear forces to the cell apex via integrin-linked magnetic beads. Both biological responses were monitored with fluorescent microscopy by labeling intracellular calcium with Fluo-3 calcium dye and by infecting cells with GFP-paxillin fusion proteins.

Monitoring calcium concentration changes proved unreliable for determining mechanotransduction thresholds, while a non-graded, time dependent (~ minutes) steady load threshold for mechanotransduction was established between 0.90 and 1.45 nN for focal adhesion site activation. Activation was greatest near the point of forcing ($< 7.5 \mu\text{m}$), indicating that shear forces imposed on the apical cell membrane transmit non-uniformly to the basal cell surface and that focal adhesion sites may function as individual mechanosensors responding to local levels of force. Results from a continuum, viscoelastic finite element model of magnetocytometry that represented experimental focal adhesion attachments provided support for a non-uniform force transmission to basal surface focal adhesion sites. Frequency variation between 0.1 and 50 Hz altered focal adhesion translocation and resulted in a biphasic response minimized at 1.0 Hz. Furthermore, applying the tyrosine kinase inhibitors genistein and PP2, a specific Src family kinase inhibitor, resulted in differential effects on force-induced translocation. These results highlight the mutual importance of force transmission and biochemical signaling in focal adhesion mechanotransduction.

Principal Thesis Supervisor: Roger D. Kamm
Title: Professor of Mechanical Engineering

Force-induced calcium concentration change and focal adhesion translocation: Effects of force amplitude and frequency

<u>Chapter 1 Introduction</u>	9
Section 1.1 Physiological significance of the endothelium	9
Section 1.2 Fluid shear stress mechanotransduction studies.....	11
Section 1.3 Physical basis for mechanotransduction	13
Section 1.4 Studying rapid biological readouts.....	19
<u>Chapter 2 Calcium concentration changes</u>	25
Section 2.1 Materials and methods	25
Section 2.2 Results	28
Section 2.3 Discussion	31
<u>Chapter 3 Focal adhesion translocation</u>	35
Section 3.1 Materials and methods	35
Section 3.2 Results	38
Section 3.2.1 GFP-expression verified with Western analysis	38
Section 3.2.2 Load magnitude affects focal adhesion translocation	39
Section 3.2.3 Quantitative analysis of loading effects.....	41
Section 3.2.4 Steady load mechanotransduction threshold.....	41
Section 3.2.5 Mechanotransduction depends on loading frequency	45
Section 3.2.6 Role of kinase signaling in focal adhesion mechanotransduction	46
Section 3.3 Discussion	49
Section 3.3.1 Steady load response characteristics.....	49
Section 3.3.2 Frequency dependence of focal adhesion translocation.....	53
Section 3.3.3 Tyrosine kinase inhibition differentially affects mechanosensing.....	55
<u>Chapter 4 Conclusions and future directions</u>	57

List of figures

Figure 1-1.	Vessel wall pathophysiology of atherosclerosis.....	10
Figure 1-2.	Decentralized description of mechanotransduction.....	13
Figure 1-3.	Intracellular calcium signaling pathways	14
Figure 1-4.	Continuum viscoelastic simulation of magnetocytometry	17
Figure 1-5.	Tensegrity interpretation of focal contact mechanotransduction	18
Figure 1-6.	Magnetic trap experimental design.....	20
Figure 1-7.	Focal adhesion protein signaling pathways	22
Figure 2-1.	Fluo-3 visualization of intracellular calcium.....	27
Figure 2-2.	Photobleaching calibration	28
Figure 2-3.	Distribution of calcium response curves	29
Figure 2-4.	Percentage of cells responding with calcium signaling.....	30
Figure 2-5.	Spontaneous calcium signaling	31
Figure 3-1.	GFP-paxillin expression verification.....	39
Figure 3-2.	Focal adhesion translocation visualization.....	40
Figure 3-3.	Baseline translocation.....	42
Figure 3-4.	Steady load mechanotransduction threshold	43
Figure 3-5.	Local versus global translocation	44
Figure 3-6.	Simulation of focal adhesion shear stress distribution	45
Figure 3-7.	Variable frequency sinusoidal force application	47
Figure 3-8.	1.0 Hz square wave force application.....	47
Figure 3-9.	Tyrosine kinase inhibition translocation.....	48
Figure 3-10.	GFP-actin visualization of stress fiber formation.....	52

Chapter 1

Introduction

Biology and engineering have merged to study mechanotransduction, the process by which cells transduce external mechanical stimuli into complex biological signals. Mechanotransduction is an essential cell function, controlling its growth, proliferation, protein synthesis, and gene expression (12, 30). Under specific mechanical environments, mechanotransduction can either protect against or promote pathological events. Extensive studies on endothelial mechanotransduction have characterized how shear stress affects signaling in endothelial cells and more recent studies have begun to look at molecular level events in response to force, but the physical basis for sensing external mechanical forces and transducing the mechanical signal into biochemical responses remain unknown. Understanding the basic mechanisms of how cells transduce mechanical forces in biological signals has implications for a broad spectrum of pathological disorders that develop in mechanically active environments. In this study, a highly controllable, local mechanical load is used to investigate early biological signals of mechanotransduction in vascular endothelial cells by monitoring intracellular calcium changes and focal adhesion dynamics.

Section 1.1 Physiological significance of the endothelium

The endothelium plays a critical role in the vasculature by creating an actively responsive cell barrier between flowing blood and the vessel wall (see Figure 1-1). Functionally, the endothelium regulates transport at the blood/vessel wall interface and responds to both the mechanical and chemical environment. During an inflammatory episode, the endothelium is chemically stimulated to express adhesion receptors that allow leukocytes to adhere to the endothelial surface (e.g. VCAM-1). Further stimulation due to continued inflammation forms stronger adhesions and leukocytes emigrate across the endothelium,

along chemoattractant gradients, and into the underlying tissue (56). Along with an active role in inflammation, the properly functioning endothelium regulates acute and chronic vessel tone in response to the shear stress environment. Endothelial-derived nitric oxide is a potent vasodilator, while prostacyclin and endothelin produced by the endothelium act as vasoconstrictors. These endothelial functions are critical for regulating the distribution of blood flow to various organs, maintaining healthy blood vessels, and protecting against vascular disease.

Genetic predisposition as well as acquired characteristics, such as high cholesterol diets, chronic smoking, and sedentary life styles contribute to several cardiovascular disorders, including atherosclerosis, diabetes mellitus, hypertension, hyperlipidemia, hypercholesteremia, and heart failure (54). The fluid shear stress environment, in addition to genetic and lifestyle factors, is a major determinant of vascular disease progression. Local regions of disturbed flow can alter endothelium-dependent vasotone in response to the mechanical environment, a chronic condition broadly classified as endothelial dysfunction (24). Clinical correlations between fluid shear stress and vascular disease progression have prompted researchers to investigate how mechanical forces influence cellular signaling (60). These investigations developed the basis for studying mechanotransduction in vascular endothelial cells.

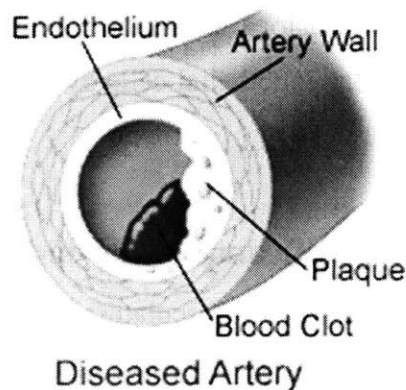


Figure 1-1 Cross sectional view of the vessel wall during the development of atherosclerotic lesions. The endothelium provides a chemical and mechanical barrier between flowing blood and the smooth muscle cell artery wall. This active barrier is at the interface of vascular disease development.

Mechanical and hemodynamic stresses on the endothelium arise from blood flow and variations in arterial blood pressure. Hemodynamic stresses on the vessel wall reduce to a shear and normal component. The normal component creates a circumferential stress on the artery wall and the shear component of hemodynamic stress acts directly on the endothelium, which then transmits it to deeper regions of the tissue. Flow remains laminar throughout the majority of the vasculature, even as the cardiac cycle oscillates pressure values, and generally maintains a positive shear stress on the vessel wall. Mean positive wall shear stress values in the larger arteries range from 10 to 30 dynes/cm² (59). Reynolds numbers predicted both experimentally with MR techniques and in computational studies are on the order of 100 (46). Flow becomes disturbed at major branches and bifurcations of the vasculature. The outer wall of these regions correlates with locations of lesion formation and plaque development. The four major locations of plaque growth include: 1) the coronary arterial bed; 2) the major branches of the aortic arch and carotid bifurcation; 3) the visceral arterial branches of the abdominal aorta; 4) the terminal abdominal aorta and its major branches. Hemodynamic analysis has characterized those regions by flow separation, recirculation, and reattachment, as well as temporal and spatial gradients in shear stress (59). These shear stress gradients lead to a low and variable shear stress on the endothelium. It is now understood that the time-varying disturbed flow and low shear stress affects endothelial cell signaling and alters the phenotype with respect to endothelial cells in high shear stress environments, all of which contribute to endothelial dysfunction and vascular disease progression (13, 24, 54, 59, 60).

Section 1.2 Fluid shear stress mechanotransduction studies

Fluid shear stress studies aimed at understanding the link between mechanical stress, cell signaling, and disease progression have used cell morphology, gene expression, and intracellular calcium concentration to characterize the effects of time-varying hemodynamic stress on endothelial cell signaling and relate the findings to vascular disease. Cells exposed to rapidly fluctuating shear stress environments, generated with turbulent flow, do not align with the direction of flow as do cells exposed to laminar fluid shear stress (15), while oscillating fluid shear stress with a low mean positive force does

not induce the same gene expression profile as flow with a high mean positive force (20, 24, 59). Furthermore, ramped levels of laminar fluid shear stress with different rates of increase result in graded nitric oxide (39) and intracellular calcium (51) responses. These seminal studies show that the biological response of a cell to mechanical force has magnitude and frequency dependent thresholds for activation and that the time course of applied external force has significant effects on the observable biological response.

Fluid shear stress studies with the endothelium have also revealed how hemodynamic shear stress can stimulate both atheroprotective and pro-atherogenic cell signaling. Nitric oxide, a potent vasoregulator that helps maintain healthy vessel tone and inhibits the expression of the leukocyte adhesion molecules, is produced in the endothelium at a rate that depends on the level of shear stress. Another atheroprotective response regulated by fluid shear stress is prostacyclin-mediated vasodilation and inhibition of cell proliferation. Conversely, cellular signaling has a pro-atherogenic effect in regions of disturbed flow and low mean shear stress. Oxidative stress, the most potent factor contributing to this affect, results from a decrease in flow-induced NO release and increased angiotensin II activity. This oxidative stress oxidizes low density lipoproteins (LDLs) and increases adhesion molecule expression, prompting an inflammatory response and altered endothelial permeability (58). Another important factor in atherosclerosis development is endothelin I release. Normally inhibited by NO release in regions of high mean shear stress, endothelin I acts as a vasoconstrictor and leads to the vessel narrowing characteristic of advanced stage atherosclerosis (59). Recent studies using DNA array technology to screen for mechanically-inducible genes have found that laminar shear stress, when compared to static or turbulent environments, down regulates more genes identified as atherogenic compared to up regulated genes (20). This finding further reveals the atheroprotective response of the endothelium.

Although fluid shear stress studies have elucidated important characteristics of mechanotransduction and vascular disease progression, namely the magnitude and time dependent components of the biological response and mechanically dependent gene expression profiles, the sensor of mechanical force that initiates biological signaling remains unknown. Further understanding of the physical basis for mechanotransduction

will provide insight into how an initial mechanical sensing event propagates into biochemical signaling cascades that alter endothelial gene expression and phenotype.

Section 1.3 Physical basis for mechanotransduction

Several spatially separated mechanosensors have been identified from experimental observations with the intent to better understand the physical basis for mechanotransduction. These mechanosensors include integrins (26, 55), cytoskeleton constituents (17, 22), G-proteins (8, 28, 45, 62), ion channels (34, 45, 62), and intercellular junction proteins (12). When studying specific mechanosensors, considerations must be made for the chemical environment, mechanosensor location, and cellular force transmission (see Figure 1-2).

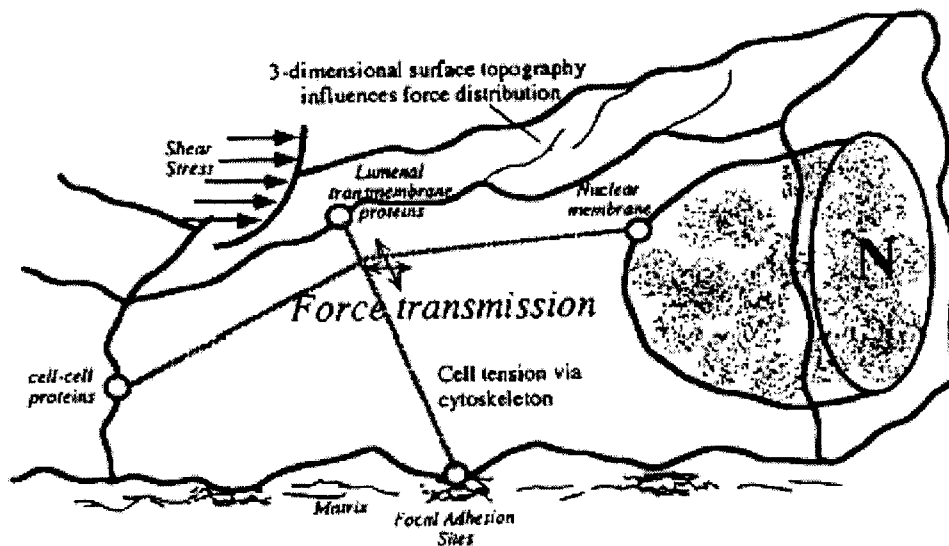


Figure 1-2 Proposed mechanosensors, including membrane biomolecules and ion channels, integrins, cell-cell adhesion proteins, the nucleus, and the cytoskeleton, occupy spatially separated regions of the cell. Due to the decentralized nature of these mechanosensors, local force transmission to specific mechanosensors significantly influences how a cell responds to external force (14).

A mechanosensor may rely on specific diffusive mediators, such as tyrosine kinases, for mechanical activation as well as the local force transmission. This sensitivity to local force transmission must be considered when choosing a mechanical probe, which significantly affects how forces transmit to discrete locations in the cell. Furthermore, justified spatial and material assumptions need to be made when choosing a material

model for estimating cellular force transmission. All of these considerations are critical for interpreting experimental observations resulting from mechanical stimulation and expanding our understanding of how cells sense and transduce mechanical forces into biochemical signals.

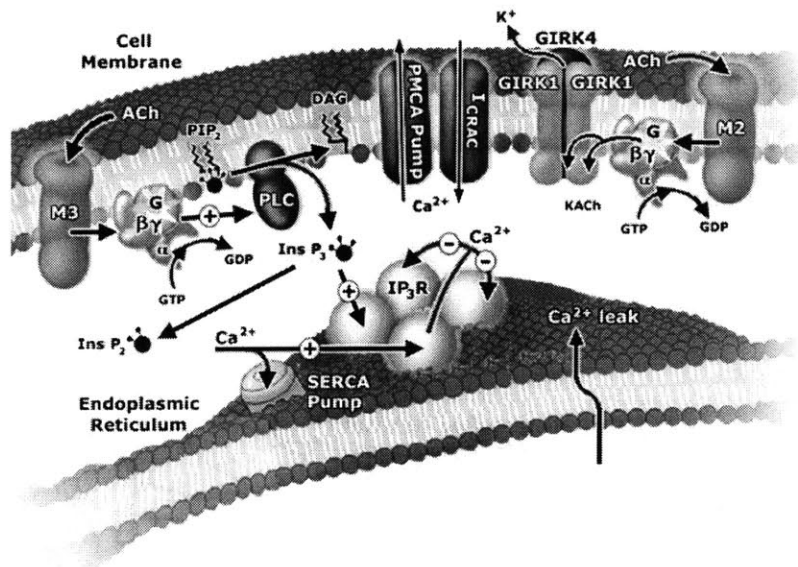


Figure 1-3 Sources of calcium concentration changes include inward calcium release calcium activated ion channels (I_{CRAC}) and the endoplasmic reticulum. Control of the chemical environment and biochemically-induced calcium concentration changes is necessary for interpreting force-induced calcium concentration changes (7).

The chemical environment can directly affect the activation and effectiveness of individual mechanosensors. When studying calcium concentration changes, it is important to control ATP and calcium ion concentration in the extracellular media. Calcium concentration changes can arise from both inward calcium ion channels and intracellular calcium release from the endoplasmic reticulum (see Figure 1-3), while ATP has been shown to chemically induce calcium fluctuations in the absence of mechanical stress (50). Interpretation of intracellular calcium concentration changes requires prior knowledge of the chemical environment in order to deduce the effect of mechanical force on specific calcium sources. The significance of chemical effects can be studied with pharmacological inhibitors that target specific biological pathways. Inhibitors may affect mechanotransduction by blocking ion channels and integrin receptors, as well as impair

kinase and protease activity and cytoskeletal integrity. Therefore, knowledge and control of the chemical environment, either by altering the presence of biomolecules or applying pharmacological inhibitors, is critical for understanding and interpreting mechanotransduction.

Force transmission across the membrane is important for ion channel, G-protein, and membrane biomolecule activation during mechanotransduction. The cellular membrane structure consists of a phospholipid bilayer, glycolipids, cholesterol, and membrane associated proteins. This phospholipid bilayer can be modeled as a two-dimensional fluid that allows membrane molecules to move by diffusion or directed motion. Intermolecular interactions, primarily hydrophobic between each leaflet of the bilayer resist extension and bending. Bilayer viscosity is the primary determinant of membrane fluidity, but the diffusion of integral membrane proteins is also influenced by the membrane-associated cortex. When thought of as a continuum, changes in membrane mechanical properties can potentially affect how cells transmit external forces and activate mechanosensors. As evidence, increases in membrane fluidity have been shown to increase basal GTPase activity and thus G-protein activation (8). Furthermore, stretch activated ion channels require a specific threshold of membrane strain for activation and force-induced increases in membrane stiffness have been experimentally shown to reduce the strain resulting from a particular level of force and diminish ion channel sensitivity (5).

Understanding membrane mechanics provides a physical basis for interpreting ion channel activation. Ion channels can either be directly coupled to mechanical forces, as shown with hair cells (34), or stretch activated (45). These mechanosensors help maintain ion homeostasis and drive biological pathways in the endothelium. Mechanical forces applied to ion channel-linked hair bundles increase tension in the elastic gates of the channel and subsequently increase the open probability of the mechanoelectric transduction channel. The greater the applied force, the greater the probability of channel opening. Studies applying a negative suction pressure to the cell membrane can control the opening of stretch-activated ion channels (41). Similarly, flow induces membrane polarity changes by independently stimulating inward rectifying K^+ channels and outward rectifying Cl^- channels (2).

New data suggest that G-proteins also have a role in regulating ion channel function, suggesting that K^+ and Cl^- ion channel activation is a downstream response to G-protein activation (22). G-protein activation has been cited as a possible mechanosensor critical in shear stress mediated intracellular calcium release, gene induction, and protein kinase regulation, such as ERK1/2 activation (14). Membrane mechanics and the effects of membrane fluidity significantly influence strain-induced G-protein activation and mechanotransduction. For instance, a strain magnitude of 10% delivered at a rate of 20% strain per second induces G-protein activation, whereas 20% strain at a rate of 0.3% strain per second and 2% strain at a rate of 20% strain per second both fail to induce activation (8). Furthermore, a decrease in membrane fluidity, such as caused by increased cholesterol deposits within the lipid bilayer, decreases the translational and rotational mobility of membrane constituents and leads to impaired G-protein activation due to impaired strain (27). Thus, changes in membrane mechanical properties directly influence G-protein activation and ultimately affect strain-induced mechanotransduction..

Similar to membrane mechanics, force transmission through the cell and cytoskeleton significantly affects individual mechanosensors such as the nucleus, cytoskeleton, and focal adhesions. Analysis of cytoskeleton structural models, either from a microstructural or continuum perspective, can provide further insight into how force transmission activates these cytoskeleton-associated mechanosensors. Force transmission to discrete locations along the cellular force transmission pathway activates mechanosensors at the luminal cell surface, cell-cell junctions, nucleus, and basal adhesions (12). This local force-dependent mechanosensor activation gives rise to the decentralized nature of mechanotransduction (see Figure 1-2). Estimates of force transmission to location-specific mechanosensors depends on the assumed mechanical description of the cell and cytoskeleton. Mechanical descriptions of the cell use both a microstructural and continuum approach. Microstructural analysis accounts for cytoskeletal inhomogeneity in constituents, such as actin filaments and microtubules (36), while a continuum approach estimates continuous mechanical properties that combine properties of the cytoskeleton, cytosol, and organelles (38).

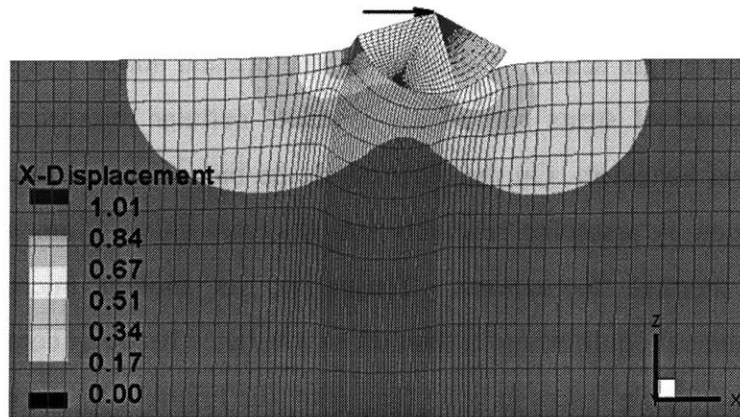


Figure 1-4 Finite element analysis estimation of cell deformation and force transmission using a continuum, viscoelastic model. The continuum description shows a decay of deformation with increasing distance from a localized load (38).

Typical continuum estimates of cellular behavior model the cell as a continuous viscoelastic material (see Figure 1-4). This accounts for the viscous energy dissipation, stress relaxation, and creep behavior observed experimentally. Viscoelastic material behavior is modeled with a combination of elastic and viscous material elements. There are three common linear viscoelastic models. The Maxwell body contains a spring and a dashpot in series, a Voight body contains a spring and a dashpot in parallel, and a standard linear solid contains a Maxwell body in parallel with a single spring. More elements can be arranged in parallel and series to account for increased viscoelastic complexity. Correlation of model estimates with experimental findings range from linear Maxwell bodies (38) to complex arrangements of elastic and viscous elements (5). Even though there is good correlation between experimental data and estimated viscoelastic material behavior, the continuum approach to cellular mechanical behavior does not account for microstructural differences in cellular constituents or microscale variations in material behavior if nanometer length scales are of interest. Also, it is important to recognize that a viscoelastic model is merely a representation of the material behavior, and the various springs and dashpots can rarely be directly connected to specific features or elements of the material they represent.

Microstructural descriptions of the cell can help in interpreting how force transmission through specific cytoskeleton constituents affects mechanosensor activation across nanometer length scales. For instance, the cellular solids model uses a repeating unit cell comprised of struts and beams to relate cellular microstructure to observed macromechanical behavior. On the other hand, the biopolymer network model predicts filament extension by assuming relatively straight cross-linked filaments and accounting for effects of thermal fluctuations. Tensegrity, yet another microstructural model, describes mechanical equilibrium in the cell as a balance between compressive forces in microtubules and tensile forces in actin filaments (see Figure 1-5), even in the absence of external force due to an internal pre-stress. Experiments have shown that twisting microbeads tethered to integrin receptors on the apical cell surface result in heterogeneous displacement of organelles at discrete locations far from the point of load application. Some view this result as force transmission through a pre-stressed cytoskeleton that lends support for a tensegrity microstructural description for mechanical cell behavior (32). Furthermore, tensegrity has been used to interpret the effects of force transmission on mechanotransduction because it describes a possible force transmission mechanism for focal stress concentration on mechanically sensitive molecules that exist within extracellular matrix adhesion sites (see Figure 1-5) and cell-cell junctions (36).

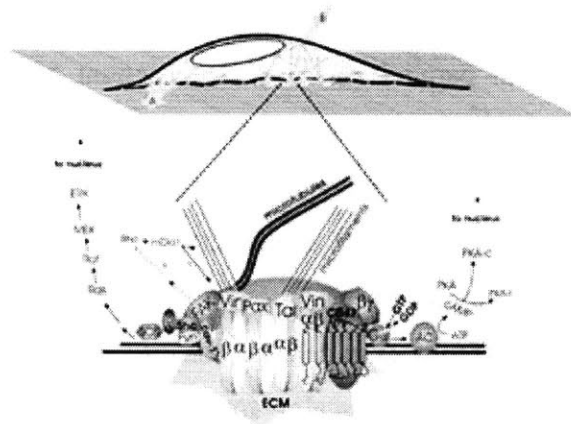


Figure 1-5 Tensegrity microstructural description of force transmission and its influence on microscale mechanotransduction. The schematic suggests that inhomogeneous force transmission through a pre-stressed cytoskeleton network concentrates at basal surface attachments and modulates integrin-associated mechanotransduction (36).

Choosing the mechanical description of the cell for a given situation depends on the deformation length scale of interest and mechanical probe size. If the probe and deformation region are both on the length scale of the spacing between cytoskeleton constituents, typically on the order of 100 nm, then a microstructural description may be necessary to provide an accurate analysis. On the other hand, if cellular deformations of interest occur over length scales significantly greater than nanometers or the length scale of the probe is significantly greater than nanometers, then a continuum description would provide an adequate estimate of force transmission. For instance, a continuum description of magnetocytometry currently provides a sufficient, experimentally verified estimate of mechanical behavior for the cell (38). However, if an accurate microstructural description for magnetocytometry existed, it would provide a better estimate of force transmission.

Section 1.4 Studying rapid biological readouts

The goal of this research was to characterize how cells sense and transduce local mechanical loads into rapid biological signals, focusing in particular on the force magnitude and frequency dependent thresholds for mechanotransduction. Addressing this goal required a rapid biological readout of mechanotransduction and a method for delivering highly controllable, localized mechanical loads to single cells. Morphological and gene expression comparisons provide a robust marker of mechanotransduction, but the response is slow, on the scale of hours, and the methods available to measure changes in molecular activity typically require large cell populations. Intracellular calcium concentration changes and focal adhesion dynamics, on the other hand, provide a rapid biological readout that can be monitored in a single cell (30, 52). Calcium concentration changes occur over the entire cell, unlike focal adhesion dynamics which occur at discrete locations along the cytoskeletal force transmission pathway. Both calcium concentration and focal adhesion readouts were used for studying force magnitude and frequency dependent thresholds in mechanotransduction, while focal adhesion dynamics provided further insight into force transmission distributions and spatial variances involved with mechanosensing.

A single pole magnetic trap was used to generate highly controllable local forces on the apical surface of individual cells (see Figure 1-6). The magnetic trap produced shear forces on the order of nano-Newtons and local stresses on the order of 100 Pa and had time variance control of load delivery, allowing for sinusoidal and square wave forcing functions. Other methods of local force application include atomic force microscopy and optical trapping, but these probes directly control deformation and not force. Forces generated with the magnetic trap act directly on single extracellular matrix ligand coated magnetic beads that bind to specific transmembrane integrins on the apical cell surface. Integrins and focal adhesion sites provide a mechanical linkage between the extracellular matrix and actin filaments of the cytoskeleton. Thus, forces applied to apical surface integrins presumably transmit directly through the cytoskeleton to basal surface adhesion sites and underlying matrix.

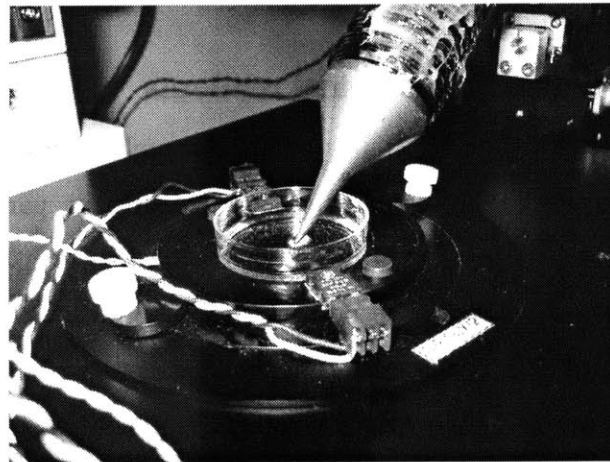


Figure 1-6. Magnetic trap used to deliver highly controllable nN-level forces to the apical cell surface via fibronectin coated microspheres.

Quantitative observations of mechanotransduction were made by monitoring intracellular calcium release and focal adhesion dynamics in response to external force. Specifically, we sought to understand the critical mechanical thresholds for signal transduction and the effects of loading magnitude, rate, and frequency, and the spatial variability of the response within a single cell. Experimental results were integrated with current finite element structural models of the cell in order to draw conclusions on how force transmission affects mechanotransduction. For calcium experiments, G-protein activation and ion channel activation are upstream events to intracellular calcium

concentration change (7). As previously discussed, membrane stiffness, bending, and deflection are thought to affect G-protein activation because G-proteins physically tether to the membrane. The majority of experiments using calcium concentration changes as a biological readout applied physiological levels of fluid shear stress and monitored changes over a population of cells. These fluid shear stress studies found a stress threshold of 0.1 dynes/cm^2 for cell activation, or roughly 10 pN per cell, with a graded response up to 4.0 dynes/cm^2 (400 pN per cell), as well as a dependence on oscillatory, non-zero mean, shear stresses (30). Single cell experiments, on the other hand, have focused on delivering forces normal to the apical cell surface to stimulate calcium ion channels (4).

Force-induced focal adhesion activation in adherent cells, as opposed to intracellular calcium release, depended on force transmission from the cell apex to basal surface via the cytoskeleton. Correlating force transmission approximations and individual focal adhesion position with activation addressed the ability of the focal adhesions to sense local levels of force. Others have used focal adhesion site remodeling as a marker of mechanotransduction, which has the advantage of being rapid, (occurring in minutes after stimulation) and site-specific. Specifically, these studies found 10% global strain (49) and 10 nN per adhesion site (48) to induce growth on the basal surface, 50 – 500 pN to initiate focal adhesion complex formation on a microbead surface (19), and 10 dynes/cm^2 fluid shear stress to direct focal adhesion translocation (42).

Integrin signaling is critical in forming and developing focal adhesion sites, as well as in recognizing external force by orchestrating mitogen-activated protein kinase activity and stress fiber formation (55). Both external and internal mechanical stress activate integrins and initiate focal adhesion reinforcement via the recruitment and binding of focal adhesion proteins (19). Src family kinase activation and tyrosine phosphorylation both have roles in early focal adhesion-associated mechanosensing (23). Phosphorylation of focal adhesion kinase (FAK) at tyrosine 397 (Tyr397) results from integrin activation and enables interaction with and activation of Src family kinase (see Figure 1-7). Src family kinase binding to FAK initiates tyrosine phosphorylation of paxillin and Cas and ultimately Rac-dependent focal adhesion turnover and cell migration (47).

Integrin activation and tyrosine phosphorylation also assist in the Rho GTPase-dependent recruitment and binding of focal adhesion proteins by regulating protein-protein interactions in proteins that contain the Src homology 2 (SH2) (44). As evidence of these interactions, cells respond to external forces with focal adhesion translocation and protein recruitment, as shown by fluid shear stress acting as a mechanotaxis stimulus to preferentially translocate focal adhesion sites in the direction of shear (42) and entire cell stretch resulting in increased focal adhesion protein recruitment (49). Cells also respond to locally applied mechanical loads, suggesting that individual focal adhesions sense local levels of force. Pico-Newton level forces applied to the apical cell surface result in focal adhesion protein recruitment to the point of load application (19). Conversely, concentrated apical surface loads on the order of 10 nN per adhesion site initiate focal adhesion complex formation and protein recruitment along the basal cell surface in regions local to the concentrated load (48). Understanding how cells transmit mechanical forces from the cell apex to basal adhesions is critical for further characterization of focal adhesion mechanosensing.

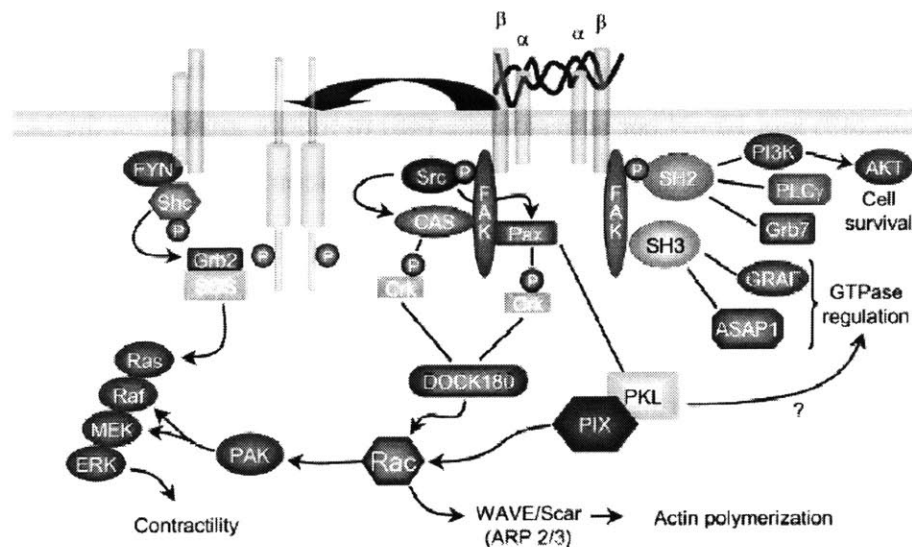


Figure 1-7. Integrin signaling upon chemical and mechanical activation that leads to tyrosine phosphorylation of focal adhesion kinase (FAK), Src family kinase activation, and downstream Rac-dependent focal adhesion turnover and cell migration, as well as Rho GTPase-dependent regulation of focal adhesion protein recruitment (47).

The following study consists of two distinct investigations, one using intracellular calcium changes as a marker for mechanotransduction and the other focusing on focal

adhesion dynamics. Quantitative analysis of intracellular calcium flux proved inconclusive. Magnetic trap loading via single magnetic beads did not consistently initiate intracellular calcium changes for a series of steady and time-varying loading magnitudes and temporal gradients, suggesting that local mechanical loads may not deliver the mechanical conditions required to activate ion channels or intracellular release pathways. Conversely, focal adhesion translocation monitoring, following the same force delivery protocols as in calcium experiments, yielded a distinct force magnitude threshold for mechanosensing. Focal adhesion translocation was monitored by expressing GFP-paxillin, a focal adhesion protein that binds to the focal adhesion targeting (FAT) region of FAK. Translocation exhibited a dependence on both the magnitude and frequency of loading, as well as Src family kinase activity and tyrosine phosphorylation, suggesting that focal adhesion mechanotransduction depends on a balance between the local mechanical stress and biochemical signaling. An understanding of how endothelial cells sense local mechanical loads via focal adhesion sites was furthered by coordinating experimental results with current cell mechanics and mechanotransduction models. Ultimately, the knowledge gained from these mechanotransduction studies will contribute to understanding mechanotransduction-linked pathologies, developing mechanical-based therapies, and engineering vascularized tissue.

Chapter 2

Force-induced calcium concentration change

The knowledge gained from mechanotransduction studies is determined by both the force applied and the biological readout monitored. For the present study, intracellular calcium concentration change was chosen as a biological readout for its rapid induction, availability of fluorescent markers, and proven response to fluid shear stress. Fundamental differences, however, exist between fluid shear stress and local load mechanotransduction that separate the two experimental designs. Most prominently, fluid shear stress studies mechanically stimulate the entire cell surface over a population of cells while magnetocytometry delivers a concentrated load to individual cells. Furthermore, single cell experiments induce responses that are direct consequences of the mechanical probe and, unlike calcium ion concentration, do not typically reflect any influence of intercellular communication. Overall, single cell experiments provide a method for isolating the role of individual cells in mechanotransduction and establishing single cell force magnitude and frequency dependent thresholds.

Section 2.1 Materials and methods

Endothelial cell culture and materials

Bovine aortic endothelial cells (BAEC) were isolated and passages 3-11 were used. Cells were cultured in Dulbecco's modified Eagle's medium (DMEM, Cambrex, East Rutherford, NJ) supplemented with 10% fetal calf serum (FCS) and 1% penicillin/streptomycin. Prior to BAEC plating, 22 mm glass cell culture dishes (WillCo Wells BV, Amsterdam, Netherlands) were coated overnight at 4°C with 2 µg/ml fibronectin (Invitrogen, Carlsbad, CA, 33016-023) in phosphate-buffered saline (PBS). BAEC were plated on the fibronectin coated glass culture dishes in 2 ml DMEM supplemented with antibiotics and 10% FCS at a density of approximately 100,000 cells/dish. After incubating overnight at 37°C, the plated cells' medium was exchanged

for fresh DMEM supplemented with 5% ITS and antibiotics in order to serum starve the BAEC and reduce the incidence of spontaneous calcium release. After 24 hours of serum starvation, fresh ITS medium containing 4 μ M Fluo-3 (Molecular Probes, Eugene, OR) calcium dye and a suspension of 4.5 μ m diameter fibronectin-coated magnetic beads (DynaL Biotech, Lake Success, NY, Dynabeads M-450) was exchanged. A broad range of commercially available calcium dyes exist, both spectral and ratiometric, that have different binding kinetics and fluorescent properties. Fluo-3, chosen for its rapid association with free calcium ions, is a spectral calcium dye with maximum excitation at 504 nm and maximum emission at 526 nm. Using spectral dyes, however, is limited by photobleaching and an uncertainty associated with calibrating intracellular ion concentrations based on fluorescent intensity levels. The final bead concentration added with Fluo-3 was approximately 1.6×10^6 beads/dish. Fibronectin coated beads presumably bind to the $\alpha_5\beta_1$ and $\alpha_v\beta_3$ integrins that transmit forces to the actin cytoskeleton network. BAEC were given a 45 minute incubation period at 37°C to allow Fluo-3 permeation and bead attachment to the cell surface before mechanical loading.

Fluorescent microscopy

Cells were imaged at 60x with an inverted light microscope (Olympus, Melville, NY, IX-70) equipped with a water immersion objective and temperature control plate and recorded with a digital camera (Roper Scientific MASD, San Diego, CA, CoolSNAP). Sub-confluent cells binding single magnetic beads were selected for experimentation (see Figure 2-1). After locating cells in the viewing window that met the experimental criteria, the magnetic trap was lowered to the bead plane. The cells were continuously imaged for 60 seconds, with a 750 ms exposure time and 250 ms delay between images. Magnetic trap force delivery was initiated after 10 seconds of imaging in order to establish a baseline fluorescent intensity.

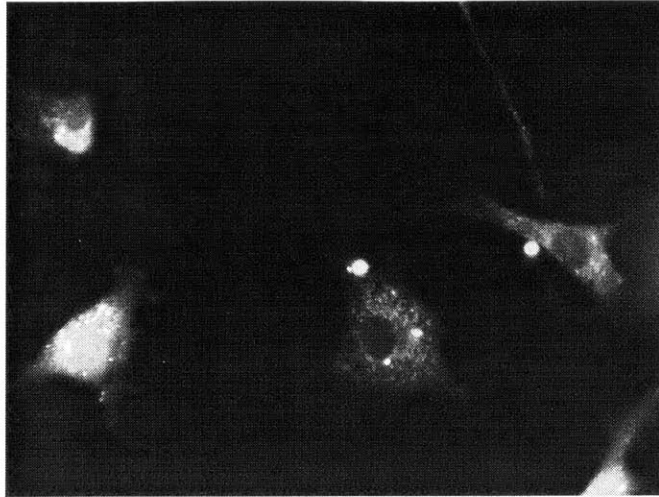


Figure 2-1. Viewing window of cells loaded with Fluo-3 calcium dye and single magnetic beads (circular bright spots). The magnetic trap was positioned at the right edge of the window, so the two cells binding magnetic beads experienced different levels of force.

Image analysis

Custom image analysis algorithms for segmenting entire cells, or portions of individual cells, and calculating the pixel-by-pixel fluorescent intensity changes were written for MATLAB (Math Works, Natick, MA). All fluorescent intensity data were normalized with respect to the initial fluorescent intensity of a given pixel. Photobleaching accounted for a significant decrease in the fluorescent intensity over the 60 second exposure. However, a photobleaching calibration was performed by calculating the change in normalized fluorescent intensity for cells binding single magnetic beads in the absence of a magnetic trap force and applying an average correction factor to the normalized intensity level based on the experimental decay. The average experimental decay with respect to time was found empirically by fitting the decay to an exponential curve (see Figure 2-2), which allowed for intensity adjustment of each experimental time point.

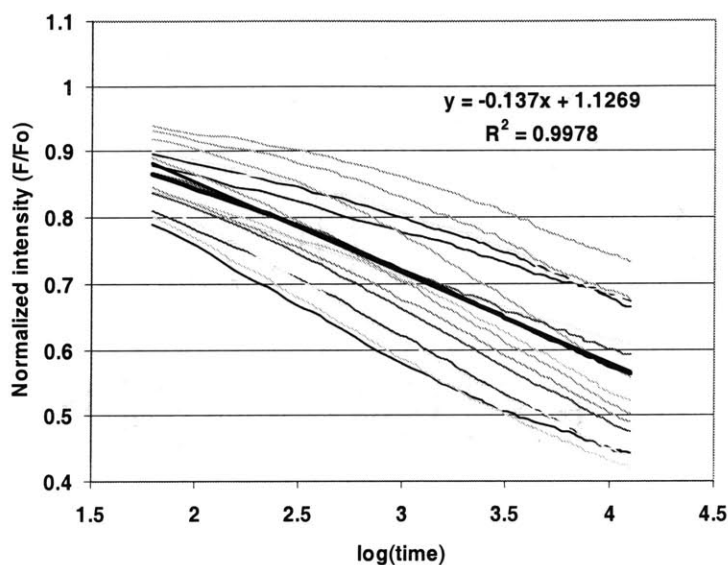


Figure 2-2. Calcium dye photobleaching calibration. The bold line indicates the average normalized intensity decay with time on a logarithmic time curve. Fitting the photobleaching intensity decay to an exponential relationship allowed for correction of the experimental fluorescent intensity profiles.

Magnetic trap force application

The magnetic trap generated both a steady and non-reversing sinusoidal shear force of varying frequency. The majority of data was obtained with a 1.0 Hz, non-reversing sinusoidal forcing function with mean positive forces ranging from 0.13 to 18.7 nN. Steady, ramp, square, and high frequency forcing functions were also used with nN-level forces. The magnetic trap force levels were calibrated by suspending the experimental magnetic beads in dimethylpolysiloxane (Sigma Aldrich, St. Louis, MO, DMPS-12 M) and monitoring the local bead velocity as the bead moved towards the magnetic trap. Using Stoke's Law for viscous drag force F around a sphere, $F = 6\pi\mu rV$, where μ is the fluid viscosity, r is the sphere radius, and V is the sphere velocity, the magnetic trap force generation was calibrated as a function of distance from the magnetic trap for a given input amperage. For more information regarding the magnetic trap design and use, refer to Huang et al. 2002 (33).

Section 2.2 Results

The results presented here correspond to calcium concentration changes in response to 1.0 Hz non-reversing sinusoidal loading. Preliminary experiments were also performed

with steady, ramp, square, and frequency varying sinusoidal loading. A 1.0 Hz sinusoidal force with a non-zero mean was chosen based on its physiologic relevance to hemodynamic shear stress and previous studies with fluid shear stress that showed endothelial cells respond to non-reversing sinusoidal loading with changes in intracellular calcium concentration (30). Furthermore, monitoring calcium concentration changes met the biological readout criterion of being rapid by responding within 40 seconds of the onset of fluid shear stress.

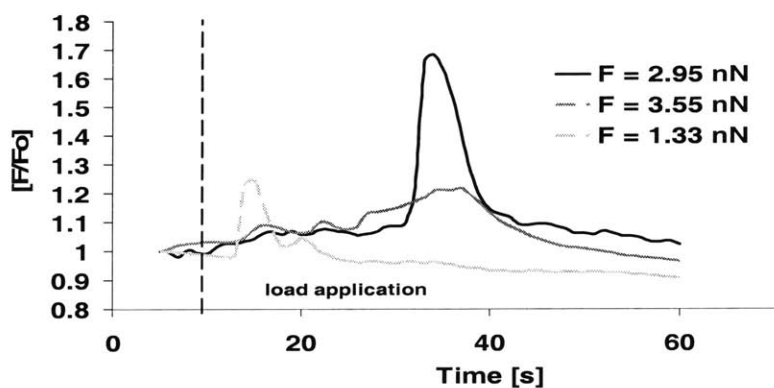


Figure 2-3. Typical distribution of calcium spikes in response to external force. The changes in calcium concentration occurred 10 – 30 seconds following the onset of force application, but have variable response profiles and maximum changes in fluorescent intensity.

Overall, 319 cells were tested using a 1.0 Hz sinusoidal forcing function with a mean positive force offset. The mean positive force on a single cell, which ranged from 0.13 to 18.7 nN, depended on the separation distance between the magnetic trap and integrin-bound magnetic bead. Cells responding to external force with a significant change in intracellular calcium, as determined by normalized fluorescent intensity increases greater than 10%, typically showed a calcium spike within 10 – 30 seconds after the onset of force and a variable time-course change in fluorescent intensity (see Figure 2-3). The force-induced calcium concentration changes were observed for loads greater than 0.91 nN, but only 7.8% of the cells tested above that value responded. Furthermore, the percentage of cells responding within a given range of forces did not increase with increasing force, suggesting a non-graded response to increased magnetic trap loading (see Figure 2-4).

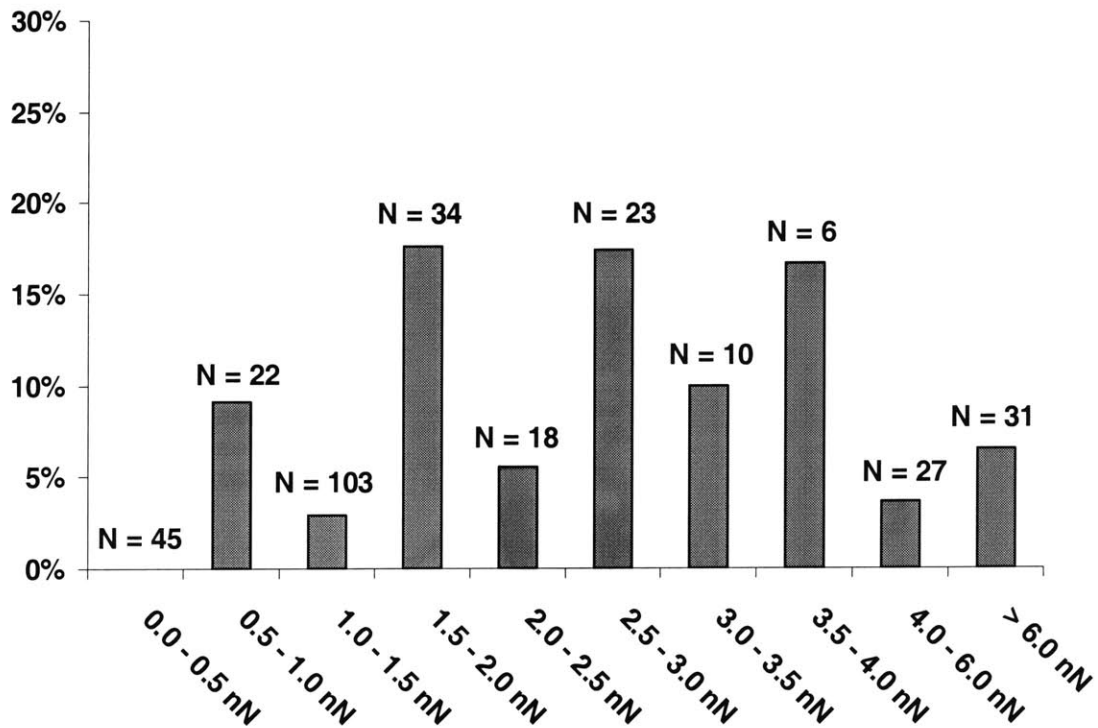


Figure 2-4. Percent of cells responding to external force with significant calcium concentration changes for a given range of mean positive force levels. All forcing functions were 1.0 Hz sine waves with the mean positive force reported. From these results, a small percentage of cells responded for all ranges of loading, but the percentage did not increase with increasing load.

Of the cells not subjected to an external force, 5.6 % responded. These spontaneous calcium responses, considered significant for a 10% increase in baseline calcium concentration, varied from slow release to rapid spike release profiles (see Figure 2-5). Based on the low percentage of cells responding to magnetic trap loading compared to spontaneous calcium signaling, calcium concentration monitoring was deemed an unreliable biological readout for single cell, magnetocytometry mechanotransduction experiments. The same unreliability and inconsistency was observed for ramp, square wave, and varying frequency sinusoidal loading.

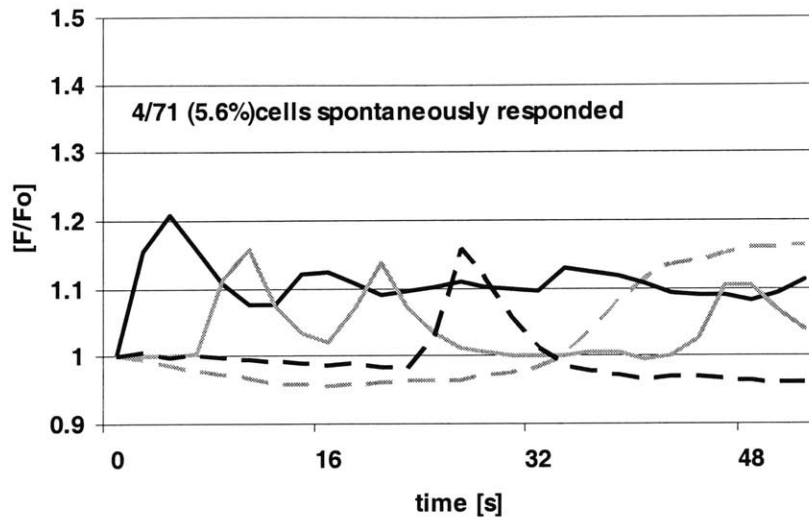


Figure 2-5. The percentage of cells showing spontaneous calcium signaling was 5.6%. Comparing this value to forced cells, in which 7.8% responded, was the basis for deeming calcium concentration changes an unreliable biological readout in magnetic trap mechanotransduction. Spontaneous calcium signaling has variable release profiles similar to forced cells.

Section 2.3 Discussion

Based on previous studies with fluid shear stress, calcium concentration changes provided a promising biological readout and marker for studying force magnitude and frequency dependent mechanotransduction, but nevertheless proved unreliable and inconsistent for single cell experiments due to the low percentage of responding cells and inseparability from spontaneous signaling. Possible explanations for this inconsistency include the initial calcium concentration being too high to detect significant changes, unsuccessful activation of the calcium release mechanosensor during localized magnetic trap loading, and the lack of cell-cell communication in single cell experiments.

The initial calcium concentration could affect both the second messenger sensitivity to calcium concentration changes and the experimental resolution in detecting fluorescent intensity changes. Others have shown that calcium signaling requires a depletion of intracellular calcium in order to sensitize the cells for calcium signaling (40). Although not calibrated for exact concentration, the single cells tested in this study all contained detectable baseline levels of intracellular calcium. It is possible that the initial level of intracellular calcium impaired, or desensitized, the calcium signaling of the cell

in response to external force. The initial intracellular calcium concentration level, if great enough, could also reduce the sensitivity associated with quantifying changes in calcium. Image analysis algorithms optimized the fluorescent intensity sensitivity by performing pixel-by-pixel normalizations on small cellular regions and reducing background fluorescence. However, a high initial calcium concentration would increase the baseline fluorescent intensity and reduce any normalized increase in calculated intensity due to mechanotransduction.

The inconsistent calcium response to external force may have also resulted from an inability of magnetic trap loading to activate the mechanosensor responsible for signaling upstream of calcium release or ion channel activation. Although the physical basis for mechanically-induced calcium signaling is not entirely known, stretch-activated ion channels (41) and G-protein activation (57) provide possible mechanosensors. Membrane mechanics affect activation in both cases. For instance, assuming that the forces transmitted through the membrane decay with distance from the point of load application, which has been shown experimentally (5), it is possible that magnetocytometry activates a smaller region of membrane-associated ion channels or only the microbead-bound integrin receptors, as opposed to fluid shear stress that acts over the entire cell glycocalyx and membrane. Stretch activated calcium ion channels have been activated with magnetocytometry, but only with a normal load applied to a large number (~ 25) of microbeads attached to the apical cell surface (4). This type of experimental loading presumably stretches a greater area of the membrane, activating more ion channels, and increasing calcium concentration changes to a detectible level. Furthermore, G-proteins tethered to the cell membrane that lead to intracellular calcium release from the endoplasmic reticulum require elevated membrane strain for activation (7, 8, 28). Thus, it is possible that G-protein and ion channel activation decrease with single cell magnetocytometry compared to fluid shear stress, due to direct loading of integrins or localized membrane strain and leading to the observed reduction in the percentage of cells responding with intracellular calcium signaling.

A final source of unreliability and the low percentage of cells responding with calcium concentration changes to an external load may be the lack of cell-cell communication. Fluid shear stress studies with endothelial cells stimulate a population of

cells by using a confluent monolayer of cells with intact communication junctions. These studies typically report a response rate of 30%, but do not discriminate between the percentage of cells directly responding to shear stress and the cells responding to cell-cell communication (51). The experiments designed in this study consciously used single cells in order to reduce the degree of uncertainty associated with a cellular response, which could have ultimately limited the percentage of responding cells compared to cells in a confluent monolayer.

Even with the inconsistencies and unreliability associated with monitoring calcium concentration changes in single cells, useful force comparisons between fluid shear stress and magnetocytometry studies can be used to infer how responding cells sense apical surface shear stress. Fluid shear stress studies typically apply shear stress on the order of 1.0 Pa, which correlates to forces on the order of 1.0 nN for a $1000 \mu\text{m}^2$ surface area cell (30, 51, 52). A concentrated 1.0 nN magnetic trap load, on the other hand, delivers a local shear stress on the order of 100 Pa based on the projected bead surface area. Magnetocytometry clearly delivers higher local stress for the same force level without inducing a calcium response, suggesting that the force magnitude or global shear stress applied across the entire cell surface is a more effective determinant of calcium signaling than the local level of shear stress. Furthermore, these data also suggest that concentrated force application to integrin receptors is not as effective as fluid shear stress at initiating calcium signaling.

Overall, monitoring intracellular calcium concentration changes proved unreliable for studying the single cell response to external force. Recent advances in molecular biology and fluorescent microscopy have enabled real-time monitoring of single proteins fused with green fluorescent protein (GFP). These protein constructs provide a promising method for studying mechanotransduction through mechanically-sensitive proteins. Focal adhesion proteins are a group of structural proteins that respond rapidly to external force by recruiting more protein and translocating (9, 48, 49). Using GFP-fusion protein techniques, the next phase of this study concentrated on monitoring focal adhesion dynamics in order to gain insight into the force magnitude and frequency dependence thresholds in mechanotransduction, as well as the effect of cellular force transmission on mechanosensing.

Chapter 3

Force-induced focal adhesion translocation

Studying mechanotransduction with changes in intracellular calcium proved inconclusive, prompting a change to focal adhesion dynamics as the biomarker of rapid mechanotransduction. As outlined in Chapter 1, focal adhesion sites provide a promising biological readout of mechanotransduction because of their mechanical force dependence during development (61), protein recruitment (49), and translocation (42). Besides the dynamic response of focal adhesion sites to both internal and external force generation, focal adhesion site dynamics provide an insightful means of studying cellular force transmission in magnetocytometry because of their spatial distribution within a single cell and seemingly individual mechanosensing capacity. Experiments monitoring rapid focal adhesion dynamics in response to local, magnetic trap loading of varying magnitude and frequency were designed for single cells in order to better understand early biological signaling and cellular force transmission effects on mechanotransduction thresholds. Furthermore, tyrosine kinase and phosphorylation signaling in focal adhesion mechanotransduction was explored by inhibiting general tyrosine kinase activity and specific Src family kinase activity. Overall focal adhesion sites appeared to function as individual mechanosensors responding to both the local mechanical and tyrosine kinase signaling stimulation.

Section 3.1 Materials and methods

Endothelial cell culture and materials

Bovine aortic endothelial cells (BAEC) were isolated and passages 3-8 were used. Endothelial cell isolation was verified with an isolectin stain (Molecular Probes, Eugene, OR, Alexa 594) by fixing the BAEC in 4 % PFA for 10 minutes at room temperature, blocking with 5 % BSA for 30 minutes at room temperature, and incubating at 37°C for 10 minutes in 1 mg/ml isolectin (neutral pH aqueous buffer). Cells were cultured in

Dulbecco's modified Eagle's medium (DMEM, Cambrex, East Rutherford, NJ) supplemented with 10% fetal calf serum (FCS) and 1% penicillin/streptomycin. Prior to BAEC plating, 22 mm glass cell culture dishes (WillCo Wells BV, Amsterdam, Netherlands) were coated overnight at 4°C with 2 µg/ml fibronectin (Invitrogen, Carlsbad, CA, 33016-023) in phosphate-buffered saline (PBS). BAEC were plated on the fibronectin coated glass culture dishes in 2 ml DMEM supplemented with antibiotics and 10 % FCS at a density of approximately 100,000 cells/dish. The plated cells were incubated overnight at 37°C.

Upon reaching ~70% confluence, the BAEC were transiently transfected with the GFP-paxillin vector (gift of K. Yamada, NIH) using FuGene6 (Roche, Indianapolis, IN) with a 3:1 transfection reagent (µl) to DNA (µg) or GFP-actin vector (Clontech, Palo Alto, CA) with a 6:1 transfection reagent (µl) to DNA (µg) ratio. Western analysis with anti-paxillin (RDI, Flanders, NJ) and anti-GFP (Sigma-Aldrich, St. Louis, MO) monoclonals verified the expression of GFP-paxillin 24 hours post-transfection. After incubating at 37°C for 24 hours, the medium was exchanged for fresh DMEM, containing 10 % FCS, antibiotics, and a suspension of 4.5 µm diameter fibronectin-coated magnetic beads (Dynal Biotech, Lake Success, NY, Dynabeads M-450). The final bead concentration was approximately 1.6×10^6 beads/dish. BAEC were given a 60 minute incubation period at 37°C to allow bead attachment to the cell surface. Src family kinase and tyrosine phosphorylation inhibition was achieved by applying 10 µM PP2 (Calbiochem, La Jolla, CA) or 100 µM genistein (Calbiochem, La Jolla, CA) during the 60 minute, magnetic bead attachment incubation period at 37°C.

Fluorescent microscopy

Cells were imaged at 60x with an inverted light microscope (Olympus, Melville, NY, IX-70) equipped with a water immersion objective and temperature control plate and recorded with a digital camera (Roper Scientific MASD, San Diego, CA, CoolSNAP). Sub-confluent cells expressing GFP-paxillin and binding a single magnetic bead were selected for experimentation. After locating a cell that met the experimental criteria, the magnetic trap was positioned 75 µm from the magnetic bead and lowered to the bead plane. A control sequence of fluorescent images was first obtained by imaging at $t = 0, 1,$

3, and 5 minutes. Following the control sequence, an external forcing function was applied and the cells were again imaged at $t = 1, 3, \text{ and } 5$ minutes. The control image at $t = 5$ minutes was used for the $t = 0$ minutes forcing sequence image. In order to ensure basal surface imaging, both the control and forcing function images were recorded as an image stack by scanning vertically $5 \mu\text{m}$ with $0.25 \mu\text{m}$ step sizes.

Image analysis

The image that best captured the basal surface focal adhesion plane was chosen for analysis after deconvolving the image stacks (VayTek, Fairfield, IA). Custom image analysis algorithms for segmenting individual focal adhesion sites and tracking the corresponding translocation vectors were written for MATLAB (Math Works, Natick, MA). Translocation vectors were calculated with respect to the initial bead position, which typically did not displace more than $\sim 1 \mu\text{m}$.

Magnetic trap force application

The magnetic trap generated both a steady and non-reversing sinusoidal shear force of varying frequency. The steady load was applied at 0.90, 1.45, and 2.25 nN force levels, while the non-reversing sinusoidal forcing functions maintained a mean of 1.45 nN with a 2.25 nN maximum force and were applied at frequencies of 0.1, 1.0, 10, and 50 Hz. A 1.0 Hz square wave was also applied with the same mean and maximum force as the sinusoidal forcing functions. The magnetic trap force levels were calibrated by suspending the experimental magnetic beads in dimethylpolysiloxane (Sigma Aldrich, St. Louis, MO, DMPS-12 M) and monitoring the local bead velocity as the bead moved towards the magnetic trap. Using Stoke's Law for viscous drag force F around a sphere, $F = 6\pi\mu rV$, where μ is the fluid viscosity, r is the sphere radius, and V is the sphere velocity, the magnetic trap force generation was calibrated. For more information regarding the magnetic trap design and use, refer to Huang et al. 2002 (33).

Computational simulations

Our viscoelastic, finite element model of the cell was extended to incorporate variable basal surface contact conditions mimicking the typical focal adhesion plane topology

observed in our experiments. The simulation assumed a continuum, incompressible, homogeneous, isotropic Maxwell viscoelastic material with a shear modulus $G = 100$ Pa and viscosity $\mu = 100$ Pa/s (characteristic time constant $\tau = 1$ s) (38). A continuum approach effectively models large scale cellular deformation distributions that exceed the length scales of individual microstructural cytoskeleton constituents without specifically assigning material properties for actin filaments and microtubules or accounting for the inhomogeneity observed by others (32). This continuum-like behavior has been verified experimentally by Karcher et al, 2003 (38). Geometrically the cell was modeled as a 20 μm radius half cylinder, either 5 μm or 3 μm high. A ramp force reaching 1.125 nN, half of the 2.25 nN experimental load, was applied to the apical cell surface over a period of 0.2 seconds. Initial simulations used a 5 μm height and constrained the entire basal cell surface in all three translational directions. Subsequent simulations were modified to better represent experimental adhesion conditions by correlating specific sets of model nodes on the basal cell surface to experimental regions of focal contact, fixing the focal adhesion site-associated nodes, and reducing the model height to 3 μm . The remaining basal surface nodes were free to translate. For simulation purposes, it was assumed that focal adhesion sites undergo negligible translocation during the 0.2 second simulation.

Statistical analysis

All data reported were collected from at least three separate experiments and reported as mean \pm SEM. Differences among experimental parameters were assessed using one and two-way ANOVA. Post hoc paired comparisons were also performed with the Bonferroni test (Prism 4.0, GraphPad Software Inc., San Diego, California, USA). Statistically significant results were considered for P values less than 0.05.

Section 3.2 Results

Section 3.2.1 GFP-paxillin expression verified with Western analysis

Cells infected with GFP-paxillin express both endogenous paxillin and exogenous GFP-paxillin. Paxillin, a 68 kDa protein, has a molecular weight of 95 kDa when fused with GFP. Western analysis was performed with both anti-paxillin and anti-GFP antibodies on samples containing only endogenous paxillin, endogenous paxillin and

GFP-fascin, and endogenous paxillin and GFP-paxillin in order to verify the expression of GFP-paxillin. All samples expressed the 68 kDa endogenous paxillin and cells infected with GFP-paxillin expressed the 95 kDa GFP-paxillin (Figure 3-1A). Western analysis with a GFP primary antibody was performed in order to confirm that the anti-paxillin antibody did not associate with GFP. Only samples containing GFP-fascin and GFP-paxillin yielded positive results, indicating that GFP-paxillin was expressed (Figure 3-1B). The phase contrast image in Figure 3-1C corresponds to the fluorescent image in Figure 3-1D, taken 24 hours post-transfection. These images show the relative transfection efficiency using GFP-paxillin.

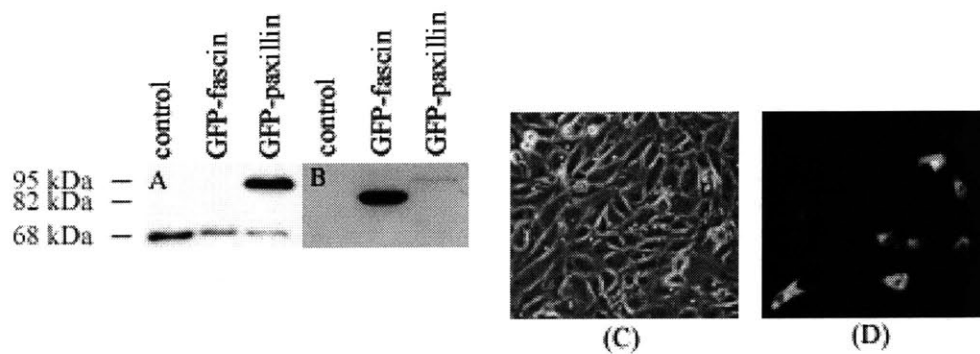


Figure 3-1. Western analysis verification of GFP-paxillin expression using (A) anti-paxillin and (B) anti-GFP. Cells transfected with GFP-paxillin expressed both endogenous paxillin (68 kDa) and exogenous GFP-paxillin (95 kDa). Comparison of the same viewing field with (C) phase contrast imaging and (D) fluorescent imaging shows the transfection efficiency.

Section 3.2.2 Load magnitude affects focal adhesion translocation

Post-processing image enhancement and analysis algorithms provided a qualitative approach to characterizing focal adhesion translocation in the presence of an externally applied force. Focal adhesion translocation was visualized by assigning single colors to fluorescent images taken at separate time points and merging the two images for comparison. Using this technique with two different colors assigned to individual time points enabled visualization of focal adhesion translocation for both non-specific migratory movement, as in control experiments, and force-induced translocation. Images merged after 5 minutes of applying 0.90 nN and 2.25 nN steady loads to the apical cell

surface show basal surface focal adhesion movement (light grey to dark grey) in response to external force application (see Figures 3-2A and 3-2C). The white arrows indicate the magnetic bead position and the direction of force application. Focal adhesion visualization was further enhanced with background correction and segmentation image processing techniques, which resulted binary equivalents to Figures 3-2A and 3-2C (see Figures 3-2B and 3-2D, respectively). Qualitatively, a 2.25 nN external steady load applied to the cell apex via cytoskeleton-connected integrins produced greater focal adhesion translocations compared to a 0.90 nN steady load (compare Figures 3-2C and 3-2D with Figures 3-2A and 3-2B). The most evident differences between these steady loads occurred in regions local to the point of load application.

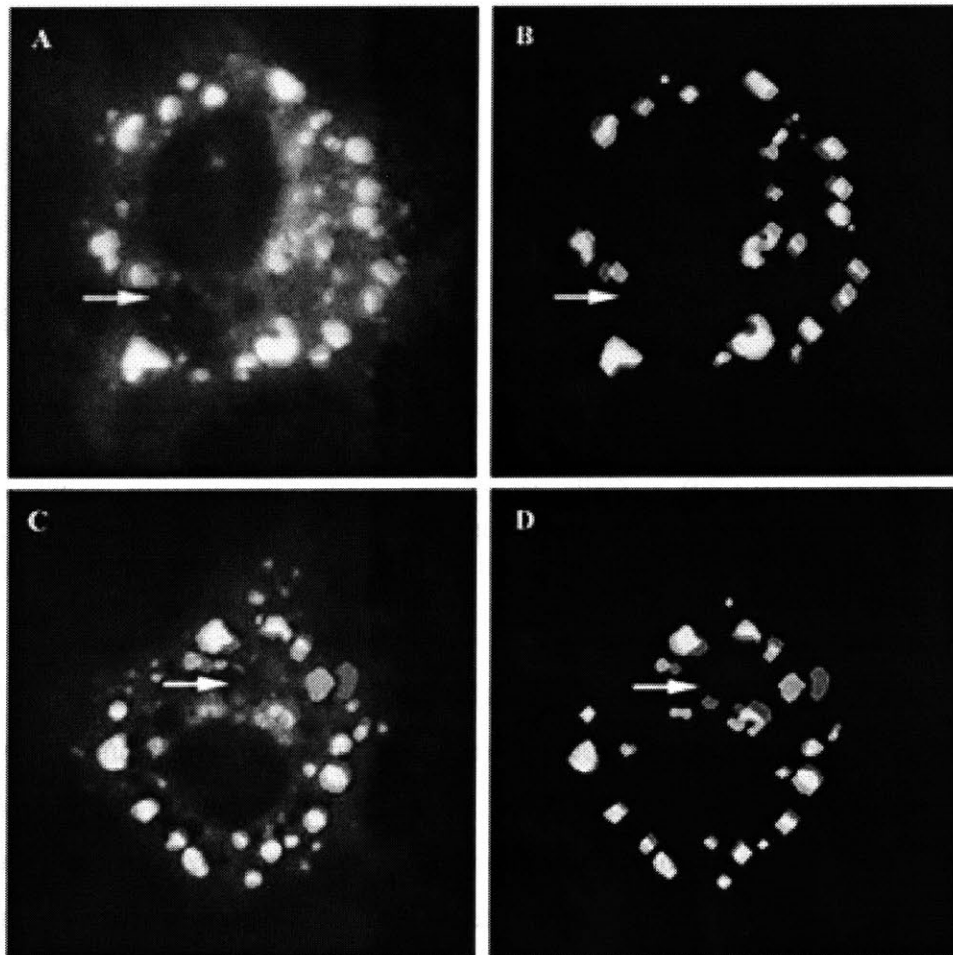


Figure 3-2. Merged focal adhesion translocation images provide visualization of focal adhesion translocation after 5 minutes (darker adhesion sites) of applying (A) 0.90 nN steady loads and (C) 2.25 nN steady loads to the apical cell surface. The magnetic bead location and direction of loading is marked by a white arrow. The 2.25 nN steady load resulted in noticeably greater translocations compared to the 0.90 nN steady load. This

effect is particularly evident near the point of load application. Image processing improved focal adhesion contrast and segmented individual sites, as in (B) and (D) which correspond to (A) and (C), respectively.

Section 3.2.3 Quantitative analysis of loading effects

The translocation of individual focal adhesion sites was quantified by calculating the centroid displacement vector between two time points. Quantitative analysis based on the average length of centroid displacement vectors shows that the magnitude and frequency of load delivery, as well as the spatial position of focal adhesion sites with respect to the point load, affects focal adhesion activation and mechanosensing.

Translocation values for the control group were measured from the same cells used in forcing experiments prior to applying the external load. Each cell contained a single fibronectin coated magnetic bead bound to its apical surface. The translocation magnitudes calculated for this control group were compared to the force-induced translocations. A second control group tested the potential effects of the magnetic field and local temperature elevation on focal adhesion dynamics. These control cells had single fibronectin coated polystyrene beads bound to their apical cell surface in order to maintain consistency with the zero force control group. Comparison of the unperturbed and magnetic field exposed control cells confirmed that the magnetic trap had negligible effects on focal adhesion translocation (Figure 3-3).

Section 3.2.4 Steady load mechanotransduction threshold

Focal adhesion translocation calculated at 1, 3, and 5 minutes during a 0.90 nN load application did not differ from control cell translocations. Increasing the steady load to 1.45 nN, however, yielded a significant increase in translocation. Translocation values at 1.45 and 2.25 nN were not significantly different, suggesting a threshold response level between 0.90 and 1.45 nN with little further change above the threshold (Figures 3-4A to 3-4C).

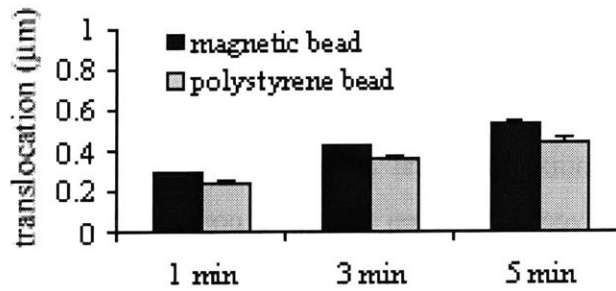


Figure 3-3. Baseline focal adhesion translocation was quantified for cells binding single magnetic or polystyrene beads coated with fibronectin. The magnetic bead control ($n = 31$ cells) established a baseline for unforced focal adhesion translocation, while the polystyrene control ($n = 4$ cells) showed a negligible contribution of the magnetic field on focal adhesion translocation.

The mechanosensing response observed for steady loads above 0.90 nN did not occur uniformly throughout the cell. Rather, translocations tended to decrease with increasing distance from the point of load application. This observation suggests that forces transmit non-uniformly to the basal cell surface and that cells contain isolated mechanosensors capable of recognizing local force levels. In order to quantify this effect, translocation was examined as a function of distance from the point of load application. For lack of a better convention, the "local" stress concentration region was estimated from a finite element model of magnetocytometry developed in our laboratory (38) and defined as a region less than 7.5 μm (radially) from the projected point of load application. The "global" region encompassed the remainder of the cell. No spatial difference in focal adhesion translocation was observed with the 0.90 nN load when comparing local and global translocation values (Figure 3-5A). On the other hand, comparison of local and global translocation magnitudes for a 1.45 nN steady load (Figure 3-5B) yielded significantly greater local translocation values. Focal adhesion translocation in the global region still significantly exceeded the control translocations.

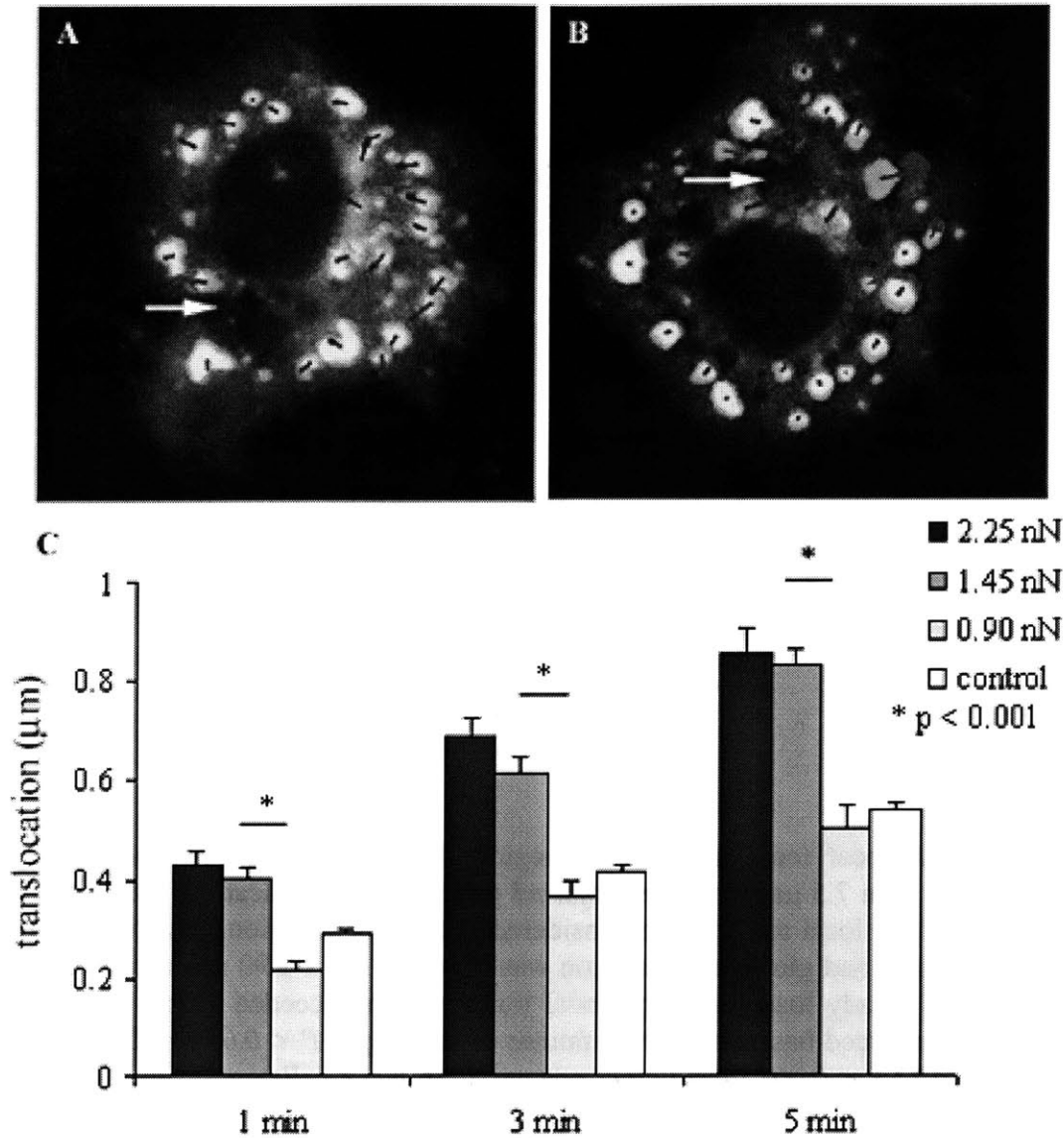


Figure 3-4. Focal adhesion displacement vectors after 5 minutes of (A) 0.90 nN steady loading and (B) 2.25 nN steady loading. The magnitude of these vectors provided a quantitative comparison of focal adhesion activation in response to external force. (C) A significant increase in translocation was found between 0.90 nN ($n = 4$ cells) and 1.45 nN ($n = 8$ cells) steady load application, defining a 1.45 nN load magnitude threshold for mechanotransduction at focal adhesion sites ($* P < 0.001$ for all time points). An insignificant difference between 2.25 nN ($n = 9$ cells) and 1.45 nN implies that the threshold is not graded.

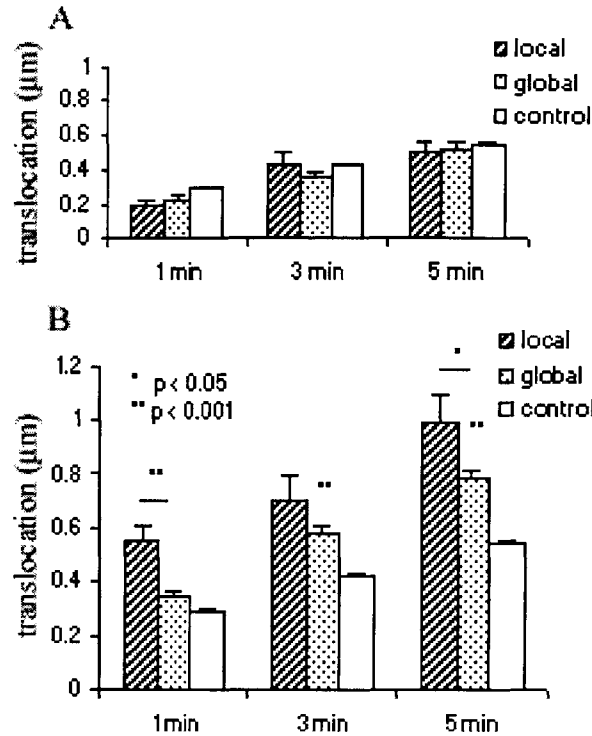


Figure 3-5. A local force transmission region was defined for focal adhesion sites positioned less than $7.5 \mu\text{m}$ from the projected point of load application. Focal adhesion sites outside of the local region were considered in the global region. (A) No significant difference in local and global translocation was observed for a 0.90 nN steady load. (B) For a 1.45 nN steady load, however, local translocation exceeded global while global exceeded the unforced baseline after 5 minutes of loading ($* P < 0.05$ for 5 minute local vs. global and $** P < 0.001$ for all other comparisons, $n = 8$ cells).

Finite element simulations correlating basal surface contact regions with experimental focal adhesion sites (Figure 3-6A) provided estimates of force transmission and shear stress distribution among basal surface focal adhesion sites. The focal adhesion site-associated nodes were fixed while the remaining basal surface nodes were free to displace (Figure 3-6B). Shear forces transmitted non-uniformly to the basal contact surface with shear stress along the basal cell surface decaying with distance from the point load (Figure 3-6C). These stress distribution estimates for steady force magnetocytometry, along with experimental data showing increased translocation in regions local to the point of load application, provide further evidence that focal adhesion sites may function as individual mechanosensors responding to local levels of force.

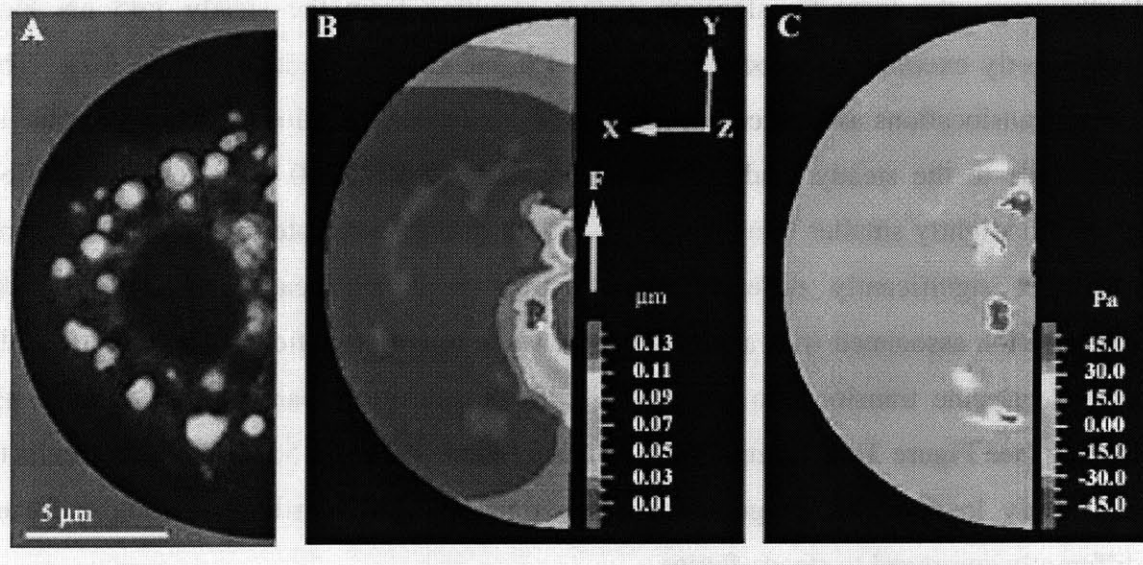


Figure 3-6. A continuum, viscoelastic finite element simulation representing experimental cell contact sites on the basal cell surface estimated the focal adhesion shear stress distribution during magnetocytometry. (A) Merged experimental fluorescent images were used to correlate focal adhesion sites to model nodes. The nodes corresponding to focal adhesion sites were fixed and the remaining nodes were free to translate. Results of the simulation show (B) zero displacement at focal adhesion site associated nodes and (C) concentrated shear stress in focal adhesion sites near the point of load application. An external load of 1.125 nN, half of the experimental 2.25 nN due to the half-cell geometry, was applied at that midpoint of the vertical edge in the positive y-direction.

Section 3.2.5 Mechanotransduction depends on loading frequency

Viscoelastic cell behavior affects how local forces transmit from the cell apex and distribute among focal adhesion contact points due to the cellular relaxation times. Effects of this behavior were examined by performing excitation frequency experiments with 0.1, 1.0, 10, and 50 Hz non-reversing sinusoidal forcing functions. All sinusoidal forcing functions contained a mean positive offset force of 1.45 nN, equivalent to the smallest steady load found to activate focal adhesion sites, a maximum force of 2.25 nN, and a minimum force of 0.75 nN. A force level centered at the threshold value was selected to accentuate the frequency dependence.

Comparison of local and global translocation magnitudes, as defined previously by a 7.5 μm radius, revealed that none of the sinusoidal forcing functions, regardless of

frequency, resulted in local region translocations that exceeded global translocations. Furthermore, the local translocation values resulting from the steady 1.45 nN load significantly exceeded the local values for 1.0 and 0.1 Hz loading (Figure 3-7). The global translocations associated with 10 and 50 Hz forcing functions were comparable in magnitude to the steady load global translocation, while the 0.1 Hz forcing function produced slightly smaller translocations. Translocations associated with 1.0 Hz forcing were not significantly different than control level translocation. Furthermore, translocation associated with a 1.0 Hz square wave forcing function did not significantly exceed baseline translocation and was significantly less compared to steady 1.45 nN loading (see Figure 3-8). Comparing the high frequency (10 and 50 Hz) forcing results to the steady load results suggests that cells transmit and transduce oscillating forces differently compared to steady forces.

Section 3.2.6 Role of kinase signaling in focal adhesion mechanotransduction

Tyrosine kinase inhibitors were applied in order to assess the role of Src family kinase activation and tyrosine phosphorylation in force-induced focal adhesion translocation. Unforced baseline translocation levels were established by monitoring translocation prior to applying a magnetic field. PP2, a Src family kinase inhibitor, resulted in a significant decrease in baseline translocation ($P < 0.0001$) when applied for 60 minutes and compared to uninhibited levels. Conversely, genistein, a less specific ATP-competitive tyrosine kinase inhibitor, did not produce a significant difference between baseline translocation when applied for the same amount of time.

After 5 minutes of loading, Src family kinase and tyrosine phosphorylation inhibition differentially affected focal adhesion translocation depending on the inhibitor, forcing frequency, and focal adhesion site location with respect to the point load. Genistein reduced both the local and global response to steady loading and the local response to high frequency loading (Figure 3-9A).

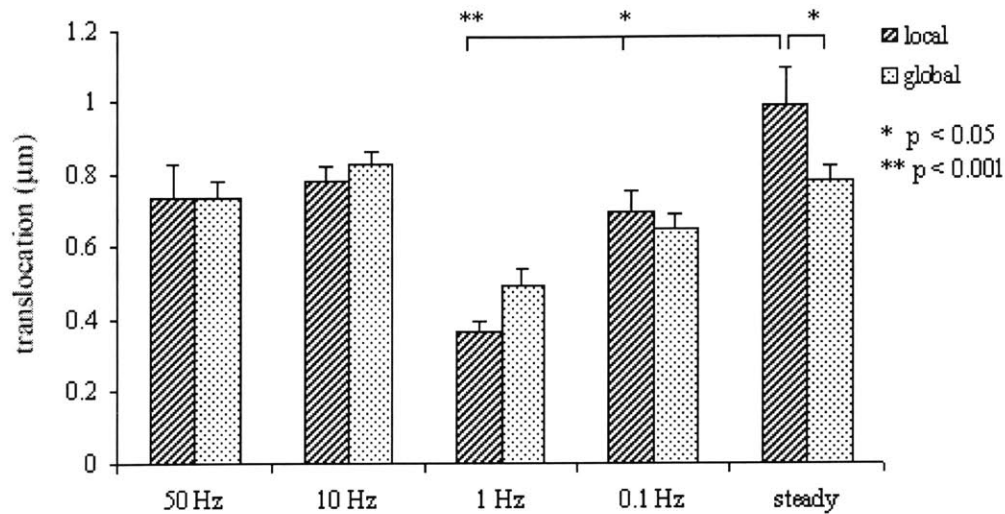


Figure 3-7. Focal adhesion translocation, both locally and globally, depends on the frequency of loading. A 1.45 nN mean positive force sinusoidal wave was applied at 0.1, 1.0, 10, and 50 Hz. Local translocation in response to 5 minute steady loading significantly exceeded the local translocation for 1.0 Hz (** $P < 0.001$, $n = 5$ cells), and 0.1 Hz (* $P < 0.05$, $n = 8$ cells) sinusoidal loading, but not high frequency 10 Hz ($n = 9$ cells) and 50 Hz loading ($n = 5$ cells). As previously shown, steady loading yielded a significant difference between local and global responses while the time varying forcing functions did not. Furthermore, neither local nor global translocation in response to 1.0 Hz sinusoidal loading significantly exceeded baseline.

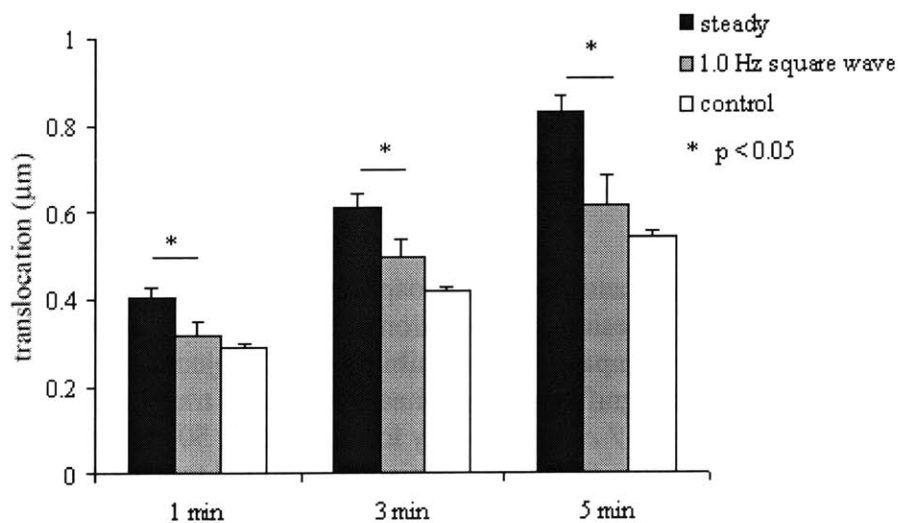


Figure 3-8. Square wave loading at 1.0 Hz with a 2.25 nN maximum and 0.75 nN minimum did not induce focal adhesion translocation significantly greater than baseline. The overall translocation magnitudes were significantly less than steady 1.45 nN loading (* $P < 0.05$, $n = 5$ cells).

PP2, on the other hand, effectively impaired translocation of global focal adhesion sites without inhibiting local focal adhesion sites from translocating significantly greater than baseline. This effect was observed for both high frequency and steady loading (Figure 3-9B). The altered levels of focal adhesion translocation resulting from tyrosine phosphorylation and specific Src family kinase inhibition imply that force-induced focal adhesion translocation depends on tyrosine phosphorylation of focal adhesion kinase (FAK), Cas, and paxillin.

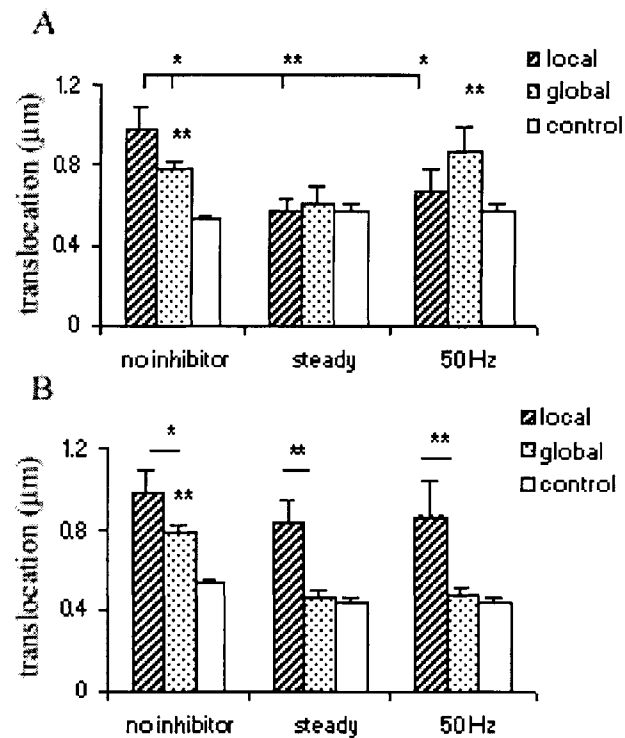


Figure 3-9. Src family kinase and tyrosine phosphorylation inhibition affects local and global force-induced focal adhesion translocation after 5 minutes of steady and high frequency force application compared to uninhibited cells subjected to 1.45 nN steady loads. (A) 100 µM genistein significantly inhibited steady load translocation both locally and globally (** $P < 0.01$, $n = 7$ cells) but only locally during 50 Hz sinusoidal loading (* $P < 0.05$, $n = 6$ cells). Lastly, the global, genistein inhibited translocation after 50 Hz loading significantly exceeded baseline (** $P < 0.01$). (B) 10 µM PP2, a specific Src family kinase inhibitor that targets focal adhesion kinase, reduced global translocation to baseline for both steady and 50 Hz sinusoidal loading, but did not affect local translocation in comparison to baseline for either forcing function (** $P < 0.001$, $n = 7$ cells for steady and $n = 4$ cells for 50 Hz; * $P < 0.05$).

Section 3.3 Discussion

Section 3.3.1 Steady load response characteristics

Force magnitude and frequency dependent thresholds for mechanotransduction were studied using focal adhesion dynamics as a measure of the cellular response to shear forces applied locally via adherent microbeads. Based on the translocation of focal adhesion sites, endothelial cells exhibit a steady force magnitude threshold for activation between 0.90 and 1.45 nN. Forces below the signal transduction threshold transmit through the cell to the basal surface without producing appreciable changes in focal adhesion translocation when compared to cells not subjected to external force. Defining the level of force required to activate a specific cellular response provides critical information for studying how cells transduce external forces into biological signals. For example, molecular simulations of protein conformational changes predict pN-level force thresholds for individual proteins, while some ion channels require nN-level forces across the cell membrane for activation (25).

The threshold reported in this study is comparable to the total integrated shear force required to activate endothelial cells with fluid shear stress. Mechanotransduction studies with fluid shear stress typically apply stresses on the order of 1 - 10 dynes/cm² (0.1 – 1.0 Pa) and observe changes in intracellular calcium and nitric oxide levels (30, 37, 39, 51), ion channel activity (2, 45), G-protein activation (28), gene expression (20), and focal adhesion translocation (42). This level of stress, applied over a typical endothelial cell area on the order of 1000 μm², results in nN-level shear forces. Similarly, nN-level lifting forces applied normal to the apical cell surface via multiple integrin linked magnetic beads induces F-actin accumulation and tyrosine phosphorylation, increasing local membrane stiffness at the bead-membrane interface as measured with atomic force microscopy (25).

Fluid shear stress studies that monitor intracellular calcium concentration changes report a stress threshold of 0.1 dynes/cm² for cell activation, or roughly 10 pN per cell, with a graded response up to 4.0 dynes/cm² (51). On the other hand, shear stress-dependent gene expression (59) and G-protein activation (28) roughly requires a shear stress of 10 dynes/cm². Our results differ in both the force-level threshold and graded response findings. Focal adhesion translocation and calcium signaling likely result from

two different mechanically activated biological pathways (11) and might therefore have two different activation thresholds. Furthermore, using single bead magnetic trap loading similar to this focal adhesion translocation study did not induce a significant change in intracellular calcium compared to unforced control cells. These findings are consistent with previous studies indicating that calcium signaling is not an essential component to focal adhesion dynamics (18) and with data from Sawada and Sheetz 2002 showing that substrate strain activates focal adhesion formation in Triton-X cytoskeletons, even in the absence of cell membranes, cytosolic-free ions and other intracellular biomolecules (49).

The increased focal adhesion translocation observed at a steady load of 1.45 nN or greater did not correlate with the direction of force application after 5 minutes. This finding is consistent with the study of Li et al. 2002 (42), who found random focal adhesion movement during the first 10 minutes of fluid shear stress application. Only after ~ 1 hour did endothelial cells subjected to fluid shear stress begin to migrate in the direction of shear force application. Furthermore, it has been shown that endothelial cells align, and actin filaments orient, with the direction of shear stress within hours of the onset of stress (3, 16). These observations suggest that the random direction of elevated focal adhesion translocation observed after 5 minutes of loading resulted from an unaligned actin filament organization characteristic of short loading times.

An insignificant change in focal adhesion area was observed after applying a steady mechanical load via fibronectin coated beads, which would have presumably corresponded to the recruitment of focal adhesion proteins. Other studies have shown that external forces, applied locally with a micropipette tip (48) and optical trap (19) or globally with fluid shear stress (42) and substrate strain (49), as well as internal myosin II-driven contractile forces, modulate focal adhesion protein recruitment that leads to focal adhesion growth (21, 61). The estimated forces required for basal surface focal adhesion growth, however, range from 3 nN (19) to 10 nN (48) per focal adhesion site in experiments with fibroblasts. Cells in the present study contained at least 10 focal adhesion sites per cell, which would correspond to forces per focal adhesion site one to two orders of magnitude smaller than the forces reported to induce focal adhesion recruitment and growth. These force-level comparisons suggest that focal adhesion

translocation is activated with externally applied forces at significantly lower levels than required for focal adhesion reinforcement.

The details of shear force transmission from the apical cell surface to the basal surface and mechanotransduction through focal adhesions are not fully understood. It is clear, however, that externally applied forces act directly on fibronectin bound integrins and transmit through the cytoskeleton to analogous basal surface attachments. The observed distribution of these forces among the numerous focal adhesions is quite complex and can apparently give rise to locally elevated stress levels even at locations relatively far removed from the site of forcing (32). In contrast, a continuum, viscoelastic description of the cell predicts that force levels decay with distance from a point load. Finite element analysis of magnetocytometry estimates a radial decay of force transmission through the cell to the basal surface for continuous basal surface constraints (38). The simulations performed for this study, with constrained basal surface regions corresponding to experimental focal adhesion sites, estimated that shear forces transmit non-uniformly to basal surface focal adhesion sites. The local focal adhesion sites with concentrated shear stress were shown experimentally to translocate significantly greater compared to global regions under steady loading conditions. Viscoelastic characterization of cellular force transmission would interpret this result as a direct consequence of focal adhesion sites sensing local levels of stress. However, focal adhesion sites in the global region still experienced translocations significantly greater in forced cells compared to non-forced cells, suggesting that soluble mechanosensing biomolecules, such as tyrosine kinases, direct focal adhesion dynamics in peripheral cell regions.

Observations that local cell stiffness increases within minutes of applying nN-level magnetic bead forces to integrin linkages (4, 25) and Pascal-level fluid shear stress (6), provide a possible biological response mechanism for local force concentration. The formation of stress fibers could increase the local cell stiffness, elevate local force transmission, and lead to more force being supported by focal adhesion sites close to the magnetic bead. Visualization of GFP-actin, however, did not show an observable increase in local stress fiber formation after 5 minutes of loading (see Figure 3-10). Consequently, the elevated focal adhesion translocation in local regions apparently did

not result from the rapid formation of local stress fibers and cell stiffening in response to a concentrated external force.

Focal adhesion sites appear to function as individual mechanosensors responding to local levels of external force, as supported by comparing local and global region translocation results. Other investigators report a similar sensing capability of focal adhesions in response to locally applied external forces (19, 48), as well as in response to local mechanical substrate properties (61). Internally generated actin-myosin II contraction also leads to focal adhesion activation (19, 21, 61). Two theories attempt to explain how focal adhesion sites sense local levels of force. The first recognizes that external forces locally perturb structural elements, making new binding partners more readily available. For example, tension induces integrin density increases at focal adhesion sites in coordination with focal adhesion site development and growth (1, 55). The second theory hypothesizes that external forces applied directly to structural proteins alter the protein conformational state, which transform the protein from an inactive state to an active state by exposing new binding sites (21). Both theories suggest an altered state of molecular-level equilibrium induces protein binding changes and subsequently initiates a cascade of local biological responses.

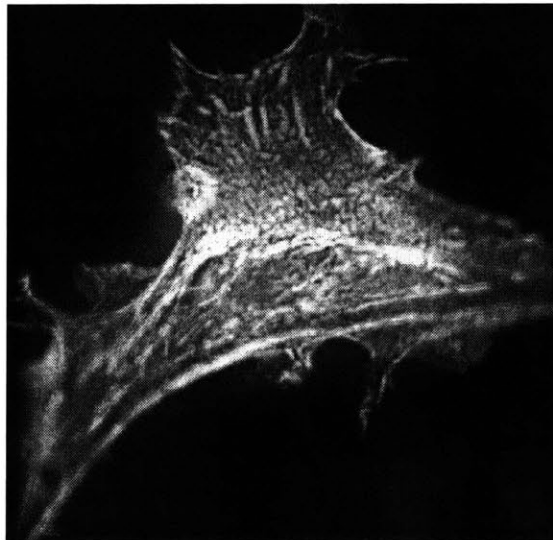


Figure 3-10. Actin stress fiber formation visualized with GFP-actin after 5 minutes of steady, 1.45 nN loading. Cells showed little change in actin organization and virtually no new stress fiber formation near the bead, suggesting that the elevated local focal adhesion response may not have resulted from rapid local stiffening of the cytoskeleton.

Section 3.3.2 Frequency dependence of focal adhesion translocation

The experiments performed with 0.1, 1.0, 10, and 50 Hz sine wave forcing functions oscillated around a mean positive force of 1.45 nN and exhibited a biphasic cellular response with a minimum at 1.0 Hz. The response to a 1.0 Hz square wave showed a similar minimum. Frequencies greater than the maximum level were limited by the magnetic trap control capabilities. Others have reported inhibited responses of cells exposed to a near-physiologic 1.0 Hz oscillating force with a positive mean when compared to steady force responses (13). This frequency dependence offers a more complex view of the cellular response to external forces. For the oscillatory forcing functions, the net time during which force levels exceeded the mechanotransduction threshold did not vary with frequency nor did the minimum and maximum force levels. However, focal adhesion translocation varied with respect to the loading rate, implying that the shear force transmission distributions at the basal surface and mechanosensing signal pathways depend on the frequency of loading.

Force transmission pathways have different relaxation time constants depending on the properties of individual structural elements, and as a result, different relative strains with frequency variations. Consider the simple viscoelastic example of a parallel, two branch system where the first branch contains a single spring and the second a spring and a dashpot in series, and acknowledge extension continuity between the two branches. In the present case of constant force amplitude, extension of the isolated spring will be greatest under a steady load or at low frequencies, and smallest at high frequencies. Conversely, the extension experienced by the spring in series with the dashpot will be smallest under a steady load and will increase to a constant, non-zero value at high frequencies. If each of the two springs represents a different force transducing element within the cell, and if the system is excited near the threshold level of extension for both of these elements, then the character of the response could vary in the manner observed in our experiments. In physical terms, the two branches of this network might be on the scale of the entire cell (e.g., the cytoskeleton and the cell membrane) or on the scale of individual molecules. Others have accounted for the differential response of cellular components by modeling the viscoelastic cellular response with multiple base units in series and parallel, where each unit consists of a single spring and a spring-dashpot

branch. These models show force transmission increases in branches as stiffness increases and that overall deformation decreases with increasing forcing frequency (43).

The biphasic response to sinusoidal forcing functions of varying frequency may have also resulted from a combination of viscoelastic force transmission characteristics and diffusive mediator effects. The transition between viscoelastic branch responses depends on the characteristic relaxation time of the model. For adherent cells the relaxation time has been shown to be on the order of one second (5, 38), which corresponds to the experimentally found minimum in focal adhesion translocation at 1.0 Hz loading. The transition between an elastic dominated and viscous dominated cell behavior may alter diffusive mediator biological signaling in focal adhesion mechanotransduction. In particular, tyrosine kinase activity has been shown to affect focal adhesion protein recruitment and site turnover, even though local force-induced structural changes mediated by talin 1 binding occur independent of tyrosine phosphorylation (23, 33). The intricate contributions of tyrosine protein kinases in focal adhesion mechanotransduction are not fully understood, but could be partially responsible for the biphasic response observed with variable forcing frequency. The 1.0 Hz sinusoidal loading minimum coincides with the physiological loading frequency of shear stress in the vasculature, suggesting that the minimum response observed could also serve an atheroprotective function. Fluid shear stress studies using a physiologic forcing frequency have shown atheroprotective gene expression profiles (20, 59), as well as minimized biologic functions (13), when compared to steady and disturbed shear stress delivery. Using focal adhesion dynamics to study atheroprotective cell mechanisms, however, would be better performed with a confluent monolayer of endothelial cells in order to minimize the migratory translocation of individual cells and allow cell-cell interactions.

The insignificant response to 1.0 Hz square wave loading may have resulted from the near-physiologic loading frequency, but could also be an effect of repeated steady force application above and below the focal adhesion translocation threshold with one second increments. The square wave essentially delivered a 0.75 nN steady load for one second followed by a one second 2.25 nN steady load. This result suggests that force-induced focal adhesion translocation depends partially on continuous mechanical

activation above a certain force threshold. Others have shown a temporal variation of mechanotransduction (18) in which different cellular responses occur after different loading times. Thus, along with the load magnitude and spatial location, the temporal component of external force delivery affects focal adhesion mechanotransduction.

Section 3.3.3 Tyrosine kinase inhibition differentially affects mechanosensing

In order to investigate the parallel effects on focal adhesion translocation of direct force transmission and tyrosine phosphorylation of focal adhesion proteins, tyrosine kinase activity was pharmacologically inhibited during steady and high frequency loading. Inhibition had both local and global effects that varied with the forcing function (see Figure 3-9).

Applying genistein, an ATP-competitive tyrosine kinase inhibitor, impaired force-induced focal adhesion translocation both locally and globally in response to steady force application and local translocation in response to high frequency (50 Hz) loading. Although others have shown that genistein selectively impairs directed endothelial cell migration under fluid shear stress depending on the temporal variation in shear stress delivery (31), the precise effects of genistein on focal adhesion mechanotransduction remain unknown. Results from tyrosine kinase inhibition with genistein, however, do suggest that diffusive mediators can differentially affect focal adhesion translocation with respect to the loading frequency by impairing integrin-mediated phosphorylation of Tyr397 on FAK (47).

PP2 is a more specific protein kinase inhibitor compared to genistein that inhibits Src family kinase activity. Application of PP2 reduced global focal adhesion translocation to baseline during both steady and high frequency loading, but did not adversely affect local force-induced translocation. PP2 has previously been shown to affect cell motility by blocking biochemically-induced focal adhesion translocation (53). It is known that Src family kinase recruitment to focal adhesion kinase induces tyrosine phosphorylation of paxillin and Cas, leading to Rac-dependent cell migration (29, 47) (see Figure 1-7). The observation that PP2 impairs global focal adhesion translocation in response to steady and high frequency loading suggests that inhibition of Src family kinase activity blocks global Rac signaling pathways that are otherwise initiated by local

force application to integrin receptors. Furthermore, in local regions of high basal shear stress where PP2 inhibition did not significantly affect translocation, the elevated focal adhesion translocation may have resulted directly from force transmission and independent of Src family kinase activity.

In summary, focal adhesion translocation resulting from mechanical stimulation has a threshold between 0.90 and 1.45 nN. The cellular response to external force depends both on the magnitude and frequency of force application. Steady load application promotes elevated local force transmission and focal adhesion translocation. At frequencies greater than 1.0 Hz, however, loading induces focal adhesion translocation of similar magnitude in both local and global regions. Furthermore, as explored with the tyrosine kinase inhibition, the mechanotransduction differences between loading patterns depends on a combination of mechanical force transmission and tyrosine phosphorylation effects. Overall these findings suggest that focal adhesion sites function as individual mechanosensors responding to local levels of force and further emphasize the intricate balance of force transmission and biochemical signaling events involved with focal adhesion mechanotransduction.

Chapter 4

Conclusions and future directions

The force level and frequency dependent thresholds involved with endothelial cell mechanotransduction, as well as the activation of discrete mechanosensors, were studied with a highly controllable local magnetic trap load. Changes in intracellular calcium concentration and focal adhesion position provided the biological readout for two distinct mechanotransduction studies. The first, which monitored intracellular calcium concentration changes, found calcium to be an unreliable and inconsistent marker for mechanotransduction in single cell experiments with a concentrated stress distribution. The second study showed focal adhesion sites have an activation threshold between 0.90 and 1.45 nN and that the response is elevated in regions local to the point of load application, suggesting that focal adhesion sites act as individual mechanosensors. Furthermore, it was shown that loading frequency and tyrosine kinase activity significantly influences the spatial response of focal adhesion sites to external force. The response characteristics of these two biological readouts highlight the differential sensitivity of biological signaling pathways to external force, while the focal adhesion dynamics study further revealed the intricate involvement of mechanical forces and biochemical signaling in a cell's response to external force.

Based on the reliability and consistency of the biological readout, focal adhesion dynamics proved more beneficial to understanding mechanotransduction. In particular, the study developed a quantitative measure of focal adhesion translocation in response to external force and altered biochemical activity, where as previous studies relied more on qualitative observations of focal adhesion dynamics (42, 61), and showed that focal adhesion sites may function as individual mechanosensors responding differentially to force magnitude and frequency. Quantitatively studying focal adhesion site translocation also provided a platform for investigating cellular force transmission, which lead to

validation of a continuum, viscoelastic model of magnetocytometry (38). In future mechanotransduction studies, further quantitative analysis should be focused on measuring changes in focal adhesion site area at the bead attachment site. An increase in focal adhesion area would indicate protein recruitment through Src family kinase activation and tyrosine phosphorylation. Others have shown that forces between 3 and 10 nN are required for basal surface focal adhesion protein recruitment, but only forces between 50 – 500 pN for vinculin recruitment to an optical bead surface (19).

Future advancements in the field of mechanotransduction will require a better understanding the physical basis for mechanical activation of specific mechanosensors. For the case of mechanotransduction through focal adhesion protein activation, and other mechanically-sensitive proteins, it is hypothesized that force-induced protein conformational changes lead to altered binding and biochemical signaling (21). Investigation of the interactions between focal adhesion proteins, either computationally with steered molecular dynamics (SMD) or experimentally by introducing two fluorescently fused focal adhesion protein to the cell, will potentially provide insight into molecular-level mechanotransduction as related to force-induced protein conformational changes.

Another critical effort in studying mechanotransduction should focus on generating a more biologically correct tissue environment. The first step to achieving a more realistic endothelial cell phenotype in these experiments would be grow the endothelial cells into a confluent monolayer and repeat the two dimensional force-induced focal adhesion translocation study. Sub-confluent endothelial cells differ from confluent endothelial cells not only because they achieve a more spread cytoskeletal configuration (35), but also because they lack cell-cell adhesion and communication. These cell-cell interactions affect all levels of function, including migration and possibly force-induced focal adhesion translocation. Force transmission in a confluent monolayer of endothelial cells may also differ compared to a single cell depending on the cytoskeleton configuration and mechanical linkage to neighboring cells. Consequently, the cell density and interconnectedness affect both the cytoskeletal structure and biochemical signaling, making it important to pursue mechanotransduction studies, both

with focal adhesion activation and other mechanosensors, using a confluent endothelial monolayer.

The next step towards engineering a more realistic endothelial cell environment involves providing an adhesion substrate with mechanical properties similar to native tissue. The morphology of focal adhesion sites associated with cells grown on compliant scaffolds would presumably differ from cells grown on glass or plastic substrates because focal adhesion sites require tension for protein recruitment, development, and maturation (61). Furthermore, it has been shown that *in vivo* three dimensional environments result in focal adhesions that differ in structure, localization, and function compared to cells grown on two dimensional rigid substrates (10). The challenge to studying focal adhesion sites on synthetic scaffolds in both two and three dimensions will involve providing a microenvironment that promotes cell adhesion, proliferation, and survival. The microenvironment includes mechanical forces, such shear stress or hydrostatic pressure, and chemical signals, such as growth factors, cytokines, oxygen, and substrate binding partners. The differential responsiveness of focal adhesions to intricate combinations of mechanical forces and soluble mediators make focal adhesion translocation monitoring a promising method for evaluating cellular function within a specific microenvironment. The knowledge gained from studying cells in mechanically and chemically controlled three dimensional environments will continue to prove critical for regenerating organs with tissue engineering.

In summary, an improved understanding of force magnitude and frequency dependent mechanotransduction was achieved by monitoring intracellular calcium concentration changes and focal adhesion dynamics. Results from this work have raised new questions about the physical basis of mechanotransduction, particularly how individual focal adhesion proteins interact and respond to force, while revealing limitations associated with current experimental biology techniques and the need for a more realistic tissue microenvironment. Ultimately, the knowledge gained from studying rapid biological readouts of mechanotransduction has implications for understanding disease development, but can also be applied to descriptions of cellular force transmission and techniques for engineering tissue.

Acknowledgements

First and foremost, I would like to thank my principal advisors, Roger and Rich, for their individual and team contributions to my thesis, education, and personal growth. Roger and Rich often presented me with two views of how to best conduct research that spanned engineering, biology, and medicine, and at the same time gave me the freedom to think on my own. For that, I am grateful. Mohammad, who also deserves recognition as an advisor, provided me with a third perspective on multidisciplinary research and I would like to thank him directly for sharing his research insight and providing life guidance.

I would also like to acknowledge members of both the Kamm and Lee labs. In the Lee lab, Jan and Jeremy for their continued image analysis and biology from an engineer's perspective guidance; Hayden for teaching me my first biology skills; Christian for his patient help with molecular biology; and the rest of the lab for their feedback, advice, and camaraderie. In the Kamm lab, Helene for her simulation assistance; Mo, Gina, Jorge, Jen, Eli, Kathie, and Hyungsuk for their entertaining conversations, ABP runs, lunch adventures, and invaluable (each in a little different way) friendships.

Lastly, I would like to thank the people close to my heart, but not from MIT. In particular, my entire family who has shown endless support and a genuine interest in understanding mechanotransduction and Christina who continually expanded my mind beyond what I learned at MIT.

References

1. **Ballestrem C, Hinz B, Imhof BA, and Wehrle-Haller B.** Marching at the front and dragging behind: differential α V β 3-integrin turnover regulates focal adhesion behavior. *J Cell Biol* 155: 1319-1332, 2001.
2. **Barakat AI, Leaver EV, Pappone PA, and Davies PF.** A flow-activated chloride-selective membrane current in vascular endothelial cells. *Circ Res* 85: 820-828, 1999.
3. **Barbee KA, Mundel T, Lal R, and Davies PF.** Subcellular distribution of shear stress at the surface of flow-aligned and nonaligned endothelial monolayers. *Am J Physiol* 268: H1765-1772, 1995.
4. **Bausch AR, Hellerer U, Essler M, Aepfelbacher M, and Sackmann E.** Rapid stiffening of integrin receptor-actin linkages in endothelial cells stimulated with thrombin: a magnetic bead microrheology study. *Biophys J* 80: 2649-2657, 2001.
5. **Bausch AR, Ziemann F, Boulbitch AA, Jacobson K, and Sackmann E.** Local measurements of viscoelastic parameters of adherent cell surfaces by magnetic bead microrheometry. *Biophys J* 75: 2038-2049, 1998.
6. **Birukov BA, Dudek SM, Verin AD, Crow MT, Zhan X, DePaola N, Garcia JG.** Shear stress-mediated cytoskeletal remodeling and cortactin translocation in pulmonary endothelial cells. *Am J Respir Cell Mol Biol* 26: 453-464, 2002.
7. **Clapham DE.** Calcium signaling. *Cell* 80: 259-268, 1995.
8. **Clark CB, McKnight NL, and Frangos JA.** Strain and strain rate activation of G proteins in human endothelial cells. *Biochem Biophys Res Commun* 299: 258-262, 2002.
9. **Critchley DR.** Focal adhesions - the cytoskeletal connection. *Curr Opin Cell Biol* 12: 133-139, 2000.
10. **Cukierman E, Pankov R, Stevens DR, and Yamada KM.** Taking cell-matrix adhesions to the third dimension. *Science* 294: 1708-1712, 2001.
11. **Davies PF.** Multiple signaling pathways in flow-mediated endothelial mechanotransduction: PYK-ing the right location. *Arterioscler Thromb Vasc Biol* 22: 1755-1757, 2002.
12. **Davies PF, Barbee KA, Volin MV, Robotewskyj A, Chen J, Joseph L, Griem ML, Wernick MN, Jacobs E, Polacek DC, dePaola N, and Barakat AI.** Spatial relationships in early signaling events of flow-mediated endothelial mechanotransduction. *Annu Rev Physiol* 59: 527-549, 1997.
13. **Davies PF, Dewey CF, Jr., Bussolari SR, Gordon EJ, and Gimbrone MA, Jr.** Influence of hemodynamic forces on vascular endothelial function. In vitro studies of shear stress and pinocytosis in bovine aortic cells. *J Clin Invest* 73: 1121-1129, 1984.
14. **Davies PF, Mundel T, and Barbee KA.** A mechanism for heterogeneous endothelial responses to flow in vivo and in vitro. *J Biomech* 28: 1553-1560, 1995.
15. **Davies PF, Remuzzi A, Gordon EJ, Dewey CF, Jr., and Gimbrone MA, Jr.** Turbulent fluid shear stress induces vascular endothelial cell turnover in vitro. *Proc Natl Acad Sci U S A* 83: 2114-2117, 1986.
16. **Davies PF, Robotewskyj A, and Griem ML.** Quantitative studies of endothelial cell adhesion. Directional remodeling of focal adhesion sites in response to flow forces. *J Clin Invest* 93: 2031-2038, 1994.

17. **Davies PF, Zilberberg J, and Helmke BP.** Spatial microstimuli in endothelial mechanosignaling. *Circ Res* 92: 359-370, 2003.
18. **Fleming I, Bauersachs J, Fisslthaler B, and Busse R.** Ca²⁺-independent activation of the endothelial nitric oxide synthase in response to tyrosine phosphatase inhibitors and fluid shear stress. *Circ Res* 82: 686-695, 1998.
19. **Galbraith CG, Yamada KM, and Sheetz MP.** The relationship between force and focal complex development. *J Cell Biol* 159: 695-705, 2002.
20. **Garcia-Cardena G, Comander JI, Blackman BR, Anderson KR, and Gimbrone MA.** Mechanosensitive endothelial gene expression profiles: scripts for the role of hemodynamics in atherogenesis? *Ann N Y Acad Sci* 947: 1-6, 2001.
21. **Geiger B and Bershadsky A.** Exploring the neighborhood: adhesion-coupled cell mechanosensors. *Cell* 110: 139-142, 2002.
22. **Geiger B, Bershadsky A, Pankov R, and Yamada KM.** Transmembrane crosstalk between the extracellular matrix--cytoskeleton crosstalk. *Nat Rev Mol Cell Biol* 2: 793-805, 2001.
23. **Giannone G, Jiang G, Sutton DH, Critchley DR, and Sheetz MP.** Talin1 is critical for force-dependent reinforcement of initial integrin-cytoskeleton bonds but not tyrosine kinase activation. *J Cell Biol* 163: 409-419, 2003.
24. **Gimbrone MA, Jr.** Endothelial dysfunction, hemodynamic forces, and atherosclerosis. *Thromb Haemost* 82: 722-726, 1999.
25. **Glogauer M, Arora P, Yao G, Sokholov I, Ferrier J, and McCulloch CA.** Calcium ions and tyrosine phosphorylation interact coordinately with actin to regulate cytoprotective responses to stretching. *J Cell Sci* 110 (Pt 1): 11-21, 1997.
26. **Goldschmidt ME, McLeod KJ, and Taylor WR.** Integrin-mediated mechanotransduction in vascular smooth muscle cells: frequency and force response characteristics. *Circ Res* 88: 674-680, 2001.
27. **Gudi S, Nolan JP, and Frangos JA.** Modulation of GTPase activity of G proteins by fluid shear stress and phospholipid composition. *Proc Natl Acad Sci U S A* 95: 2515-2519, 1998.
28. **Gudi SR, Clark CB, and Frangos JA.** Fluid flow rapidly activates G proteins in human endothelial cells. Involvement of G proteins in mechanochemical signal transduction. *Circ Res* 79: 834-839, 1996.
29. **Hanks SK, Ryzhova L, Shin NY, and Brabek J.** Focal adhesion kinase signaling activities and their implications in the control of cell survival and motility. *Front Biosci* 8: d982-996, 2003.
30. **Helmlinger G, Berk BC, and Nerem RM.** Calcium responses of endothelial cell monolayers subjected to pulsatile and steady laminar flow differ. *Am J Physiol* 269: C367-375, 1995.
31. **Hsu PP, Li S, Li YS, Usami S, Ratcliffe A, Wang X, and Chien S.** Effects of flow patterns on endothelial cell migration into a zone of mechanical denudation. *Biochem Biophys Res Commun* 285: 751-759, 2001.
32. **Hu S, Chen J, Fabry B, Numaguchi Y, Gouldstone A, Ingber DE, Fredberg JJ, Butler JP, and Wang N.** Intracellular stress tomography reveals stress focusing and structural anisotropy in cytoskeleton of living cells. *Am J Physiol Cell Physiol* 285: C1082-1090, 2003.

33. **Huang H, Dong CY, Kwon HS, Sutin JD, Kamm RD, and So PT.** Three-dimensional cellular deformation analysis with a two-photon magnetic manipulator workstation. *Biophys J* 82: 2211-2223, 2002.
34. **Hudspeth AJ.** Hair-bundle mechanics and a model for mechano-electrical transduction by hair cells. *Soc Gen Physiol Ser* 47: 357-370, 1992.
35. **Ingber DE.** Tensegrity II. How structural networks influence cellular information processing networks. *J Cell Sci* 116: 1397-1408, 2003.
36. **Ingber DE.** Tensegrity: the architectural basis of cellular mechanotransduction. *Annu Rev Physiol* 59: 575-599, 1997.
37. **Jow F and Numann R.** Fluid flow modulates calcium entry and activates membrane currents in cultured human aortic endothelial cells. *J Membr Biol* 171: 127-139, 1999.
38. **Karcher H, Lammerding J, Huang H, Lee RT, Kamm RD, and Kaazempur-Mofrad MR.** A three-dimensional viscoelastic model for cell deformation with experimental verification. *Biophys J* 85: 3336-3349, 2003.
39. **Kuchan MJ and Frangos JA.** Role of calcium and calmodulin in flow-induced nitric oxide production in endothelial cells. *Am J Physiol* 266: C628-636, 1994.
40. **Kwan HY, Leung PC, Huang Y, and Yao X.** Depletion of intracellular Ca²⁺ stores sensitizes the flow-induced Ca²⁺ influx in rat endothelial cells. *Circ Res* 92: 286-292, 2003.
41. **Lansman JB, Hallam TJ, and Rink TJ.** Single stretch-activated ion channels in vascular endothelial cells as mechanotransducers? *Nature* 325: 811-813, 1987.
42. **Li S, Butler P, Wang Y, Hu Y, Han DC, Usami S, Guan JL, and Chien S.** The role of the dynamics of focal adhesion kinase in the mechanotaxis of endothelial cells. *Proc Natl Acad Sci U S A* 99: 3546-3551, 2002.
43. **Mazzag BM, Tamareisis JS, and Barakat AI.** A model for shear stress sensing and transmission in vascular endothelial cells. *Biophys J* 84: 4087-4101, 2003.
44. **Miyamoto S, Teramoto H, Coso OA, Gutkind JS, Burbelo PD, Akiyama SK, and Yamada KM.** Integrin function: molecular hierarchies of cytoskeletal and signaling molecules. *J Cell Biol* 131: 791-805, 1995.
45. **Nakao M, Ono K, Fujisawa S, and Iijima T.** Mechanical stress-induced Ca²⁺ entry and Cl⁻ current in cultured human aortic endothelial cells. *Am J Physiol* 276: C238-249, 1999.
46. **Paley M, Hose R, Marzouqa I, Fenner J, Wilkinson I, Noguchi Y, and Griffiths P.** Stable periodic vortex shedding studied using computational fluid dynamics, laser sheet flow visualization, and MR imaging. *Magn Reson Imaging* 18: 473-478, 2000.
47. **Parsons JT, Martin KH, Slack JK, Taylor JM, and Weed SA.** Focal adhesion kinase: a regulator of focal adhesion dynamics and cell movement. *Oncogene* 19: 5606-5613, 2000.
48. **Riveline D, Zamir E, Balaban NQ, Schwarz US, Ishizaki T, Narumiya S, Kam Z, Geiger B, and Bershadsky AD.** Focal contacts as mechanosensors: externally applied local mechanical force induces growth of focal contacts by an mDia1-dependent and ROCK-independent mechanism. *J Cell Biol* 153: 1175-1186, 2001.
49. **Sawada Y and Sheetz MP.** Force transduction by Triton cytoskeletons. *J Cell Biol* 156: 609-615, 2002.

50. **Shen J, Gimbrone MA, Jr., Lusinskas FW, and Dewey CF, Jr.** Regulation of adenine nucleotide concentration at endothelium-fluid interface by viscous shear flow. *Biophys J* 64: 1323-1330, 1993.
51. **Shen J, Lusinskas FW, Connolly A, Dewey CF, Jr., and Gimbrone MA, Jr.** Fluid shear stress modulates cytosolic free calcium in vascular endothelial cells. *Am J Physiol* 262: C384-390, 1992.
52. **Shen J, Lusinskas FW, Gimbrone MA, Jr., and Dewey CF, Jr.** Fluid flow modulates vascular endothelial cytosolic calcium responses to adenine nucleotides. *Microcirculation* 1: 67-78, 1994.
53. **Shikata Y, Birukov KG, Birukova AA, Verin A, and Garcia JG.** Involvement of site-specific FAK phosphorylation in sphingosine-1 phosphate- and thrombin-induced focal adhesion remodeling: role of Src and GIT. *Faseb J* 17: 2240-2249, 2003.
54. **Shimokawa H.** Primary endothelial dysfunction: atherosclerosis. *J Mol Cell Cardiol* 31: 23-37, 1999.
55. **Shyy JY and Chien S.** Role of integrins in endothelial mechanosensing of shear stress. *Circ Res* 91: 769-775, 2002.
56. **Springer TA.** Traffic signals on endothelium for lymphocyte recirculation and leukocyte emigration. *Annu Rev Physiol* 57: 827-872, 1995.
57. **Stehno-Bittel L, Krapivinsky G, Krapivinsky L, Perez-Terzic C, and Clapham DE.** The G protein beta gamma subunit transduces the muscarinic receptor signal for Ca²⁺ release in *Xenopus* oocytes. *J Biol Chem* 270: 30068-30074, 1995.
58. **Steinberg D.** Atherogenesis in perspective: hypercholesterolemia and inflammation as partners in crime. *Nat Med* 8: 1211-1217, 2002.
59. **White, Dusserre, and Frangos.** Mechanotransduction in Endothelial and Inflammatory Cells. In: *Molecular Basis for Microcirculation Disorders*, edited by Schmid-Schonbein GW: Springer Verlag Inc, 2003, p. 640.
60. **Younis HF, Kaazempur-Mofrad MR, Chung C, Chan RC, and Kamm RD.** Computational analysis of the effects of exercise on hemodynamics in the carotid bifurcation. *Ann Biomed Eng* 31: 995-1006, 2003.
61. **Zamir E, Katz M, Posen Y, Erez N, Yamada KM, Katz BZ, Lin S, Lin DC, Bershadsky A, Kam Z, and Geiger B.** Dynamics and segregation of cell-matrix adhesions in cultured fibroblasts. *Nat Cell Biol* 2: 191-196, 2000.
62. **Zou H, Lifshitz LM, Tuft RA, Fogarty KE, and Singer JJ.** Visualization of Ca²⁺ entry through single stretch-activated cation channels. *Proc Natl Acad Sci U S A* 99: 6404-6409, 2002.